END

FILMED

MICROCOPY RESOLUTION TEST CHART

NATIONAL BUREAU OF STANDARDS-1963-A

AD _____

TECOM No.   7-CO-RD4-DPO-007

DPG Document No.   DPG-TR-85-204

TECHNICAL REPORT

NOTES ON ATMOSPHERIC STABILITY, TURBULENCE,
AND ITS MEASUREMENT

CHRISTOPHER A. BILTOFT

Meteorological Branch
Test Design and Analysis Division
Materiel Test Directorate

US ARMY DUGWAY PROVING GROUND

DUGWAY, UT 84022

MARCH 1985

DTIC
SELECTED
JUN 1 2 1985
G

APPROVED FOR PUBLIC RELEASE; DISTRIBUTION UNLIMITED

85   5   20   199

Accession For

'TIS GRA&I	☒
DTIC TAB	☐
Unannounced	☐
Justification	

By_____
Distribution/
Availability Codes

Dist	Avail and/or Special
A/1	

REPORT DOCUMENTATION PAGE		READ INSTRUCTIONS BEFORE COMPLETING FORM
1. REPORT NUMBER	2. GOVT ACCESSION NO. AD·A155 230	3. RECIPIENT'S CATALOG NUMBER
4. TITLE *(and Subtitle)* NOTES ON ATMOSPHERIC STABILITY, TURBULENCE, AND ITS MEASURMENT		5. TYPE OF REPORT & PERIOD COVERED Technical Report
		6. PERFORMING ORG. REPORT NUMBER DPG-TR-85-204
7. AUTHOR(*s*) Christopher A. Biltoft		8. CONTRACT OR GRANT NUMBER(*s*)
9. PERFORMING ORGANIZATION NAME AND ADDRESS US Army Dugway Proving Ground ATTN: STEDP-MT-DA-M Dugway, UT 84022		10. PROGRAM ELEMENT, PROJECT, TASK AREA & WORK UNIT NUMBERS 3552515201
11. CONTROLLING OFFICE NAME AND ADDRESS US Army Dugway Proving Ground Dugway, UT 84022		12. REPORT DATE March 1985
		13. NUMBER OF PAGES 56
14. MONITORING AGENCY NAME & ADDRESS*(If different from Controlling Office)*		15. SECURITY CLASS. *(of this report)* UNCLASSIFIED
		15a. DECLASSIFICATION/DOWNGRADING SCHEDULE

16. DISTRIBUTION STATEMENT *(of this Report)*

Approved for public release; distribution unlimited.

17. DISTRIBUTION STATEMENT *(of the abstract entered in Block 20, If different from Report)*

18. SUPPLEMENTARY NOTES

19. KEY WORDS *(Continue on reverse side if necessary and identify by block number)*

Richardson Number	friction velocity	stability
Obukhov length	roughness length	
Gaussian diffusion	similarity	
K-theory	turbulent kinetic energy	
turbulence	meteorological instrumentation	

20. ABSTRACT *(Continue on reverse side if necessary and identify by block number)*

Modernization of Dugway's diffusion test capabilities include the procurement of state-of-the-art instrumentation and an upgrade in data collection methodology and modeling. Dispersion of a buoyant, passive plume is due to transport by mean atmospheric motions. Although K-theory and Gaussian diffusion equations are burdened by restrictive assumptions, these equations offer the most practical means of modeling the effects of turbulence on diffusing material.

BLOCK 20. ABSTRACT (cont'd)

Turbulence occurs as vortex stretching in a sheared environment causes an energy cascade towards progressively smaller eddy sizes until viscous dissipation occurs. Direct turbulence measurements require an assortment of instrumentation due to the range of eddy sizes. Consequently, it is most economical to estimate turbulence from stability parameters and most models accept such turbulence estimators as input. The Obukhov Length, a stability parameter obtained from principal turbulent kinetic energy components, can be obtained from tower profile data using flux-gradient relationships.

LED scintillometers, acoustic sounders, radiometers, precision thermometers, and sonic anemometers are needed to upgrade Dugway's turbulence measurement capabilities. Data from these instruments will help define test go/no-go conditions, improve quality control, enhance posttest analysis capabilities, and provide improved input for diffusion modeling.

NOTES ON ATMOSPHERIC STABILITY, TURBULENCE, AND ITS MEASUREMENT

TABLE OF CONTENTS

ACKNOWLEDGEMENTS

EXECUTIVE SUMMARY

This document examines some basic relationships between atmospheric diffusion, turbulence, and stability. It lists the measurements required for an adequate description of the atmosphere for diffusion applications and the types of equipment needed for obtaining these measurements.

A substance released into the atmosphere is dispersed by atmospheric motions. Turbulent motions determine the rate of spread of the material. Mean motions transport the material downwind. Dispersion involves scales of motion ranging from the wavelengths of light (measured in micrometers) to synoptic-scale motions (measured in many kilometers).

Creation of turbulence begins when the incoming flux of solar radiation is absorbed by the earth's surface and part of it is reradiated as heat. This causes thermal discontinuities near the ground. These discontinuities and friction from the interaction of surface roughness elements and viscous forces in the atmosphere produce heat and momentum gradients. These gradients cause nonequilibrium conditions where energy is transported and dissipated through turbulent motions. Once created, turbulent eddies gradually break down into smaller eddies until they are so small that viscous dissipation into heat occurs. This process of turbulence creation and destruction continues until the driving energy is removed from the system.

Adequate description of a passive substance diffusing into a turbulent atmosphere requires a wide variety of meteorological measurements and algorithms. The Navier-Stokes equations used to describe the turbulent atmosphere are not amenable to direct solutions. Certain simplifying assumptions allow limited solutions that can yield diffusion equations used to model the turbulent atmosphere. The sophistication and accuracy of the models vary with the amount of detailed turbulence measurements or calculations available and the degree of realism of the algorithms used.

Several forms of information can be used in turbulence models. The most direct form is turbulence measurements. However, these may not be available because of time, cost, or logistic problems. Also, most models lack the sophistication required to handle detailed turbulence data. Turbulence can also be described as a function of stability, the best estimates of which are ratios of heat and momentum fluxes derived from the principal components of the turbulent energy equation. Profile measurements of wind and temperature provide mean wind and temperature model input data and are used for calculation of gradients. If fluxes of heat and momentum are assumed to remain essentially constant within the surface boundary layer, flux/gradient relationships provide a direct means of calculating stability from profile measurements. The Obukhov Length is an excellent stability parameter for use in turbulence models. It is derived from the turbulent kinetic energy equation with a minimum of qualifying assumptions and can be reliably obtained from high quality wind and temperature profile measurements.

An adequate description of atmospheric turbulence will require a variety of meteorological instruments. Sets of pyranometers and pyrgeometers are needed for measurement of fluxes of long and shortwave radiation through a surface. Scintillometer measurements of refractive index structure near the ground will supply information on eddy activity in the viscous dissipation

range. Micrometeorological anemometer cups and vanes and precision thermometers, at logarithmically-spaced height intervals from 2 to 16 meters, are the most reasonable source of profiles of mean wind and temperature. Instruments capable of measuring high-frequency fluctuations could provide data for turbulence spectrum analysis. Correct combinations of these instruments could provide data on the fluxes of heat, momentum, and moisture. Acoustic sounders can provide in-depth measurements of wind, estimates of bulk turbulence, and information on the depth of convection or mixing layers. Scintillometers can provide the possibility of calculating path-averaged wind and divergence. An expanded, improved mesonet grid and thorough modernization of the weather station would provide the meso- and synoptic-scale information needed to describe the setting in which turbulence events occur.

The information will be most useful if the instruments are deployed and the data collected, analyzed, and entered into the model by people with a firm understanding of the assumptions used and knowledge of the limitations of the site and conditions of data collection. When the data are collected at sites approximately homogeneous in space and with meteorological conditions stationary in time, turbulence can be described as a function of stability. Significant departures from these conditions vastly complicate data interpretation. Stability parameters can be used as test go/no-go criteria, for test data quality control, and for modeling. If data from the instruments discussed above were available, in-depth posttest analysis would be possible.

1. INTRODUCTION:

Diffusion meteorologists agree that behavior of a plume released into the atmosphere is controlled by meteorological influences. Unless the release is accompanied by the emission of a tremendous amount of heat, initial source characteristics are quickly overwhelmed and plume behavior becomes a function of the motions in the atmosphere into which the plume is released. The mean wind field transports the released material downrange and turbulent motions cause horizontal and vertical spreading of the material. Transport is a function of mean wind fields that are readily measured. Diffusion is a function of turbulent eddies that are much more subtle and difficult to quantify.

A basic equation describing concentration (χ, mg/m^3) of an inert, non-depositing material, diffusing at distance x (meters) downwind from a continuous ground level gaseous point source, over a surface homogeneous in space, into an atmosphere stationary in time is

$$\chi = Q/(\pi \ \sigma_y \ \sigma_z \bar{\bar{u}}), \qquad (1.1)$$

where Q is the source strength in mg/sec, σ_y and σ_z are the crosswind and vertical plume standard deviations and u is the transport wind speed. The $\sigma_y \sigma_z u$ in Equation 1.1 is proportional to the volume occupied by the diffusing material, assuming normal or Gaussian distribution. Derivation of this result is performed in Section 4 of this document. The double overbar on transport wind speed indicates that it is a mean wind speed averaged over travel time and depth of the cloud. Equation 1.1 quickly becomes complicated as different source configurations or chemical reactions occur, or as atmospheric characteristics change.

Pasquill (1976) discusses σ_y, the horizontal component of cloud growth, as a function of downwind travel distance and measured standard deviation of the horizontal wind angle (σ_A), as expressed by equation 1.2.

$$\sigma_y = \sigma_A \ x \ f(x) \qquad (1.2)$$

Equation 1.2 applies to a stationary wind field free of horizontal and vertical wind shears. These conditions can be approximated within the first several tens of meters above ground level and over travel times of several tens of minutes. The function $f(x)$ assumes a value of unity near the source and decreases as a function of travel distance and meteorological variables.

The σ_A in Equation 1.2 is the horizontal wind angle standard deviation, a bulk turbulence parameter obtained from turbulence measurements. It should represent the integral of horizontal turbulent fluctuations over the entire spectrum of eddy sizes for a given time. In practice, the measurement is limited on the low frequency (large eddy) side by sampling duration and is

limited on the high frequency (small eddy) side by instrument response charac-
teristics and data sampling rate. Other factors affecting the magnitude of
σ_A are adequacy of instrument response characteristics and instrument
exposure.

Algorithms comparable to Equation 1.2 are available for describing σ_z,
the vertical measure of cloud growth, as a function of x. The most useful of
these algorithms include the description of σ_z as a function of the vertical
component of turbulence, represented as the vertical wind angle standard devi-
ation, σ_e.

The scales of motion that consist of eddies somewhat smaller than the
diffusing cloud contribute most significantly to diffusion through the σ_A
and σ_e terms. Scales of motion larger than the cloud tend to move the cloud
as a whole. Turbulent eddy activity near the earth's surface is the sum of a
dynamic or mechanical component generated by wind blowing over roughness ele-
ments (e.g., trees) and a convective component caused by buoyancy. The neu-
tral or adiabatic atmosphere contains only the mechanical turbulence component
where eddy activity depends on the interaction of wind with surface roughness.
Diabatic atmospheres also include buoyant low-frequency eddies, in the un-
stable case, and an assortment of high-frequency eddies superimposed on inter-
mittent low-frequency waves in the stable case. Algorithms pertaining to the
neutral through unstable diabatic atmosphere near the surface will be primar-
ily addressed because these are the conditions under which most current test-
ing is done at US Army Dugway Proving Ground (DPG), Utah.

Just as diffusion calculations require specification of the turbulence
field, turbulence can either be measured or estimated from a similarity
theory. Surface layer similarity theory is a collection of dimensional and
physical arguments that permit description of turbulence as functions of a
stability parameter. Stability parameters are combinations of pertinent
variables used to describe the degree of departure from the adiabatic condi-
tion. The usefulness of stability parameters is a function of the accuracy
with which they can be calculated and how well they represent actual
conditions.

This document describes some elementary relationships between atmospheric
diffusion, turbulence, and stability parameters derived from similarity argu-
ments. The purpose is to examine these relationships, determine the measure-
ments required for an adequate description of the atmosphere for diffusion
applications, and suggest the types of equipment that can be used to obtain
these measurements.

2. A DEFINITION OF TURBULENCE:

The coordinate system shown in Figure 2.1 is used in the following discus-
sion: The x axis is positive to the right, the y axis is positive towards the
top of the page, and the z direction is a perpendicular directed out of the
page. Components of the wind (u, v, and w) are defined along the x, y, and z
axes, respectively. The mean wind flow is assumed to be to the right along
the x axis. Vector quantities are indicated with an arrow overbar ($\rightarrow$).

The stress tensor or shear stress (τ) is defined as a force per unit area applied in normal or tangential components to a surface. Figure 2.1 shows a volume with stress tensors applied to an xy plane (constant z surface). For a viscous fluid, there are nine stress components, three on each plane. Tensors τ_{zy} and τ_{zx} operate in the xy plane, while τ_{zz} is normal (90°) to the xy plane. The first stress tensor subscript indicates the face on which the stress acts and the second subscript indicates the direction of stress action. With inviscid or frictionless fluids, the tangential stress components are zero. Then the normal stress tensor, acting in tension, is opposed by pressure forces only. By convention, tension is designated as positive and pressure (P_{zz}) as negative. For a Newtonian viscous fluid, which the atmosphere approximates, momentum transfer caused by an applied tangential stress is proportional to the rate of strain (or momentum gradient). For a Newtonian viscous fluid moving horizontally above a stationary boundary, the stress (τ_{zxo}, τ_{zyo}) is proportional to the rate of strain ($\partial u/\partial z$ or $\partial v/\partial z$) as expressed in Equation 2.1.
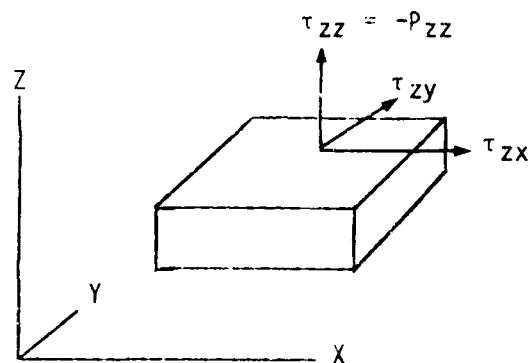
Figure 2.1. Coordinate System.

$$\tau_{zxo} = \mu \; \partial u/\partial z, \quad \tau_{zyo} = \mu \; \partial v/\partial z \tag{2.1}$$

where μ is a constant of proportionality known as the coefficient of viscosity. The subscript o on τ_{zxo} and τ_{zyo} denotes the fact that these tangential viscous terms arise because of the motions of a viscous fluid above a stationary surface. In the atmosphere, viscous terms are small except near a surface where the velocity gradient is large or at the high frequency end of the turbulence spectrum. The x component of viscous force per unit mass on a volume of air is then represented as in Equation 2.2.

$$Fx = (1/\rho) \; \partial \tau_{zxo}/\partial z = (\mu/\rho) \; \partial^2 u/\partial z^2. \tag{2.2}$$

3

The stress terms described above are used in Navier-Stokes equations which express Newton's Second Law for motion in a Newtonian viscous fluid. For the u component of an incompressible viscous fluid, the instantaneous equation of motion is

$$du/dt = (-1/\rho)\partial P/\partial x + f_c + (\mu/\rho)[\partial^2 u/\partial x^2 + \partial^2 u/\partial y^2 + \partial^2 u/\partial z^2]. \qquad (2.3)$$

Equation 2.3 presents acceleration of the u component of the wind as the resultant of pressure gradient force, Coriolis force, and viscous forces. All forces in Equation 2.3 are per unit mass. The full vector form of the equation of motion is used in Section 5 for deriving the turbulent kinetic energy equation. Normally, the rate of change in vertical wind speed gradients greatly exceeds horizontal accelerations, that is

$$\partial^2 u/\partial z^2 \gg \partial^2 u/\partial x^2, \partial^2 u/\partial y^2 \qquad (2.4)$$

and these smaller terms in Equation 2.3 can be neglected. Similar equations can be written for the v and w wind components.

In addition to the equation of motion, a statement of continuity is required to describe the action of turbulence. The equation of continuity is most easily visualized by examination of flow through a unit volume (Figure 2.2).
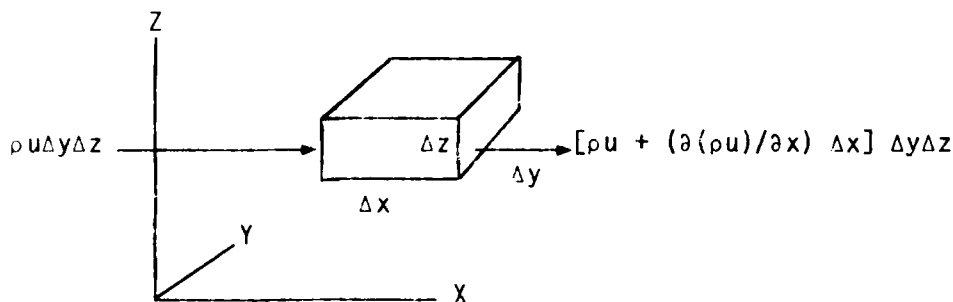
Figure 2.2   Flow Through a Unit Volume.

In Figure 2.2 consider mass inflow (ρu) multiplied by unit area $\Delta y \Delta z$ and mass outflow as $\rho + (\partial(\rho u)/\partial x)\Delta x$ where $(\partial(\rho u)/\partial x)\Delta x$ expresses changes that take place while the fluid passes through the volume. Then, the net rate of mass inflow per unit volume equals the local rate of change of density, as given in the three-dimensional mass divergence equation (continuity equation),

$$-\partial \rho/\partial t = \partial(\rho u)/\partial x + \partial(\rho v)/\partial y + \partial(\rho w)/\partial z = \nabla \cdot \rho \vec{V}. \qquad (2.5)$$

4

Equation 2.13, neglecting the total derivative and viscous terms, then becomes

$$(1/\bar{\rho})\, \partial P/\partial x - f_c = (1/\bar{\rho})[\, \partial(\bar{\rho}K_m\, \partial\bar{u}/\partial x)/\partial x +$$

$$\partial(\bar{\rho}K_m\, \partial\bar{u}/\partial y)/\partial y + \partial(\bar{\rho}K_m\, \partial\bar{u}/\partial z)/\partial z\,] \qquad (4.9)$$

and solutions are possible with the assumption that K_m is some known function along each axis. Similar expressions for heat can be written with the K-theory relationship

$$\overline{w'\theta'} = K_h\; \partial\bar{\theta}/\partial z, \qquad (4.10)$$

where θ represents potential temperature.

In the early years of diffusion work, the magnitude of K for each application was generally unknown. Because of this, the "Reynolds Analogy" was frequently employed. This analogy assumed equivalence of the diffusivities for momentum, heat, and suspended material, i.e ,

$$K_m = K_h = K \text{ material} \qquad (4.11)$$

Several problems with this analogy are:

a. Momentum transfer occurs as the result of pressure forces which do not operate equivalently on fields of heat or suspended material.

b. A material released into the air at a temperature different than the air temperature will undergo displacements relative to ambient eddy motions.

c. Any diffusing material motions caused by heating, evaporation, radiation absorption, or differential motions caused by inertial or aerodynamic effects (settling of droplets, sailing of spores, etc.) will affect diffusivity.

d. Diffusivity gradients may also be caused by terrain or roughness elements which cause shears, vortex shedding, or wake flows.

It is, therefore, generally accepted that

$$K_m \neq K_h \neq K \text{ material} \qquad (4.12)$$

K is called a coefficient of eddy diffusivity. The concept of K arises from an assumption that the mixing of eddies in the atmosphere is analogous to molecular mixing. Mixing on the molecular scale occurs as molecules travel over a characteristic molecular length scale defined as a mean path distance (ℓ) before colliding with other molecules. Bradshaw (1971) points out several problems with the analogy:

a. Turbulent eddies are continuous and contiguous, whereas gas molecules are discrete and collide only at intervals.

b. Although molecular free paths are small compared to the dimension of the flow, turbulent eddies are not.

In spite of these deficiencies, the mixing length analogy and the resultant eddy diffusivity or K-theory relationships remain popular because they provide the simplest solutions to diffusion problems. Alternative numerical methods are beyond the means and requirements of most operational diffusion programs.

Unfortunately, all the complexities of turbulent interactions influence the magnitude of K. Adequate specification of K is difficult because it is a complex function of height above the surface and stability. It also varies with the characteristics of the diffusing substance to be treated. The most familiar forms of K are those for momentum and heat. This is because wind and temperature are the most frequently measured atmospheric variables. The turbulent transfer coefficient for momentum (K_m) is defined as the product of a characteristic eddy velocity and a characteristic eddy length scale, e.g.

$$K_m \equiv (\overline{w'w'})^{\frac{1}{2}} \ell \tag{4.7}$$

Similar turbulent transfer coefficients or eddy diffusivities can readily be defined for sensible heat (K_h), moisture (K_1), or fractional atmospheric components (K material).

An example of K-theory utility is the "first order closure" or eddy diffusivity (K) closure solutions to the Navier-Stokes equations (Equation 2.13), where eddy stress is expressed directly in terms of gradients obtained from the mean motion field. Neglecting the viscous terms ($\mu/\rho\partial^2\overline{u}/\partial z^2$) and assuming that the total change with respect to time (du/dt) is zero, Equation 2.13 is reduced to a balance between the pressure gradient forces, the Coriolis term, and Reynolds stresses. K-theory relates Reynolds stresses to mean gradients using an analogy to viscous stresses in a Newtonian fluid. Equation 4.8, for example, relates $\overline{u'w'}$ to the vertical gradient of wind.

$$\overline{u'w'} = (\overline{w'w'})^{\frac{1}{2}} \ell \, \partial\overline{u}/\partial z = -K_m \, \partial\overline{u}/\partial z \tag{4.8}$$

17

The existence of sources or sinks which cause variability in Q has been difficult to quantify. Variations in Q may be due to deposition, physical, or chemical changes. A diffusion model must account for these changes to satisfy continuity, and a number of schemes are available to do this. For some trials a "budget" is obtained by passing a diffusing cloud through a vertical sampling array, which collects a series of point samples to be used to back calculate Q. Such sampling procedures tend to be elaborate and involve considerable expense. Also, cloud growth rates constrain this procedure to use near the source. Another approach is to take advantage of modern tracer technology. Modern tracers are inert, nontoxic gases that have low background concentrations and are readily measured to low concentrations. When released in a known ratio with other substances, these tracers can be used to evaluate the presence of sources or sinks for the substance being tested. Remote sensing techniques such as lidar scanning may also help resolve source strength measurement problems.

Assuming nondivergence of the mean component, as in Equation 4.3, the total derivative of $\bar{\chi}$ with the nonzero mean components from Equation 4.2 becomes

$$-d\bar{\chi}/dt = -[\partial\bar{\chi}/\partial t + \bar{u}\ \partial\bar{\chi}/\partial x + \bar{v}\ \partial\bar{\chi}/\partial y + \bar{w}\ \partial\bar{\chi}/\partial z]$$

$$= \partial(\overline{u'\chi'})/\partial x + (\overline{v'\chi'})/\partial y + \partial(\overline{w'\chi'})/\partial z \tag{4.4}$$

At this point, K-theory or gradient transfer theory is used to obtain an operational solution for some models. The alternatives are cumbersome numerical techniques that require extensive computer time and have not demonstrated practical utility in solving diffusion problems. With K-theory, it is assumed that the flux of a substance across a fixed surface can be expressed in terms of the mean gradients of that substance normal to the surface, with a diffusivity term acting as a constant of proportionality. For example, the first term on the right in Equation 4.4, $(u'\bar{\chi}')$ can be expressed by

$$\overline{u'\chi'} \simeq - K_x\ \partial\bar{\chi}/\partial x, \tag{4.5}$$

Where K_x is the diffusivity coefficient along the x-axis.

Analogous expressions are readily found for the other components. Replacing the eddy flux terms with gradient transfer forms, the right side of Equation 4.4 becomes

$$d\bar{\chi}/dt = \partial(K_x\ \partial\bar{\chi}/\partial x)/\partial x + \partial(K_y\ \partial\bar{\chi}/\partial y)/\partial y + \partial(K_z\ \partial\bar{\chi}/\partial z)/\partial z \tag{4.6}$$

16

accumulated dose, etc. The remainder of this section will discuss only χ in its relation to diffusion equations, because sampling techniques are beyond the scope of this document.

Consider a fractional component or "pollutant" emanating from a point or line source in the atmosphere. At the source, the concentration approaches infinity $(\chi_0 \to \infty)$ and at infinite distance from the source, the concentration approaches zero $(\chi_\infty \to 0)$. At intermediate distances, the gradients $\partial\chi/\partial x$, $\partial\chi/\partial y$, and $\partial\chi/\partial z$ are finite in the x, y, and z directions. Within these limits, a statement of continuity for an incompressible fluid analogous to Equation 2.5 pertains,

$$-\partial\chi/\partial t = \partial(u\chi)/\partial x + \partial(v\chi)/\partial y + \partial(w\chi)/\partial z = \nabla\cdot\chi\vec{V} = \vec{V}\cdot\nabla\chi + \chi\nabla\cdot\vec{V}. \quad (4.2)$$

The χ in Equation 4.2 is composed of a mean $(\bar{\chi})$ component representative of the average concentration in the volume of interest, and a deviation (χ') due to eddies carrying different concentrations as they move through a measured volume. The product of the fluctuating (u', v', w') component with χ' represents a flux through the volume. As before, average values of fluctuating components are zero, but correlated products of fluctuating components are nonzero.

At this point the first set in a series of assumptions are made:

a. The assumption of nondivergence is applied to the mean concentration component.

$$\bar{\chi}(\partial\bar{u}/\partial x + \partial\bar{v}/\partial y + \partial\bar{w}/\partial z) = \bar{\chi}\nabla\cdot\vec{V} = 0. \quad (4.3)$$

b. Density is assumed to be constant. Variations in χ are then essentially caused by varying amounts of the fractional component, not by changes in air density.

c. It is assumed that there are no additional sources or sinks for the fractional component, i.e., Q remains constant.

Measurements should be made in every diffusion test to check the degree of conformity of actual conditions with these assumptions. Divergence computations from path-averaged wind measurements could verify the first assumption. If possible, the divergence computation should be made on length and time scales similar to the scale of the diffusion test. Although the magnitude of divergence does not directly enter the diffusion equations used to model trial results, the presence of significant divergence could explain some of the deviations of the actual measurements from expected results.

Density is easily monitored as a function of temperature and pressure. Density variations at a specific site during a test series are usually inconsequential. However, density differences must be considered when test results from different sites or under significantly different meteorological conditions are compared.

15

$$u_2/u_1 = (z_2/z_1)^m \qquad (3.14)$$

where m is some fractional exponent. Exponent m assumes a value near 0.14 for the neutral case, but varies with stability, site roughness, and height of measurement above the surface. Exponent m is difficult to specify accurately because its magnitude is influenced by many different factors. This is unfortunate because small variations in m cause large changes in u_2/u_1. In spite of these limitations, power law formulations are popular because they provide the simplest solutions to diffusion equation wind profiles. An accurate specification of m for diffusion tests requires continuous, representative readings of wind profiles through the depth of a diffusing cloud. Remote wind sounding techniques are well suited to provide these data within the lower troposphere.

4. K-THEORY AND GAUSSIAN DIFFUSION:

With a basic definition of turbulence and two approaches to SBL wind profiles at hand, it is now appropriate to examine some basic diffusion relationships. This is not a critical examination of diffusion models, for which many references exist. This is a discussion of some of the assumptions used, but frequently not noted, in the process of developing models or designing diffusion test programs. Suggestions are also made concerning measurements necessary to verify assumptions and conduct satisfactory diffusion tests.

The quantity of airborne material is frequently described or measured as a fractional component of the air in units of parts per million or similar units easily converted to a mixing ratio (R). For example, the National Institute of Occupational Safety and Health/Occupational Safety and Health Act (NIOSH/OSHA) Pocket Guide to Chemical Hazards (Mackison and Stricoff, 1980) describes permissible exposure limits for pollutants in this form. However, diffusion equations require introduction of fractional components in terms of a concentration (χ) with units of (milli)grams per cubic meter, or related units. The conversion from R to χ is achieved by multiplying the number of (milli)grams of fractional component per gram of air by air density [in (milli)grams per cubic meter],

$$\chi = R\rho. \qquad (4.1)$$

R is usually measured by instruments which must sample over finite time intervals. When sampling duration must be considered, the units of measure become a time-averaged concentration or a dosage (dd) with units of (milli)gram·minutes per cubic meter. Also, a measure of the total accumulation of a fractional component over a period of time per unit area is often desirable. The lungs, for example, act as collecting devices, accumulating inhaled components over time. Many deposition or impaction type samplers operate in this fashion, but with varying efficiencies, yielding a measure of total accumulated dose (D) with units of (milli)grams. Total dose samplers are usually fairly simple collection devices, but their efficiencies are complicated by factors such as wind speed, angle of exposure to the wind, particle size,

14

The diabatic influence function accounts for nonlinearities in the logarithmic wind profile, caused by thermal stratification. For neutral conditions $\phi_m = 1.0$ and $\psi = 0.0$. Table 3.1 gives sample values of ϕ_m and ψ as functions of the stability parameter z/L (defined in Section 6).

Table 3.1. Dimensionless Shear (ϕ_m) and the Diabatic Influence Function (ψ) as Functions of the Stability Parameter z/L for the Unstable Case.

z/L	ϕ_m	ψ
0.0	1.000	0.000
-0.1	0.795	0.271
-0.2	0.707	0.442
-0.5	0.586	0.765
-1.0	0.500	1.084
-5.0	0.339	2.023

The boundaries of the SBL, where stress remains nearly constant and the logarithmic law applies, can be defined. The lower boundary is z_0, the top of the viscous sublayer where viscous shear becomes dominant at the expense of turbulent shear stress. Garratt (1980) finds that viscous effects distort the wind profile for heights in the range $1 < z/z_0 < 100$ and suggests a method to compensate for this effect. The upper boundary is the top of the SBL. The top of the SBL is somewhat arbitrarily defined as the height at which τ departs from τ_0 by more than 20 percent. For a representative u_* of 50 cm sec^{-1} and density held constant at 0.0012g cm^{-3}, τ_0 has a value of 3.0 g cm^{-1} sec^{-2}. Using Equation 2.13 and ignoring the viscous term, non-accelerating components are in balance when $(-1/\rho)\partial P/\partial x$ and f_c are equal and of opposite sign. Then, accelerations (du/dt) are due to spatial changes in Reynolds stress terms. If changes in the horizontal stress components are neglected (as assumed earlier), accelerations are balanced by changes in stress with height. A typical wind speed change of 1.0 m sec^{-1} in 10 minutes produces a du/dt of 0.167 cm sec^{-2}. At this rate, stress remains within 20 percent of τ_0 for 30 meters. It can be generally assumed that constant stress and the logarithmic wind profile are useful at DPG in the layer ranging from a few centimeters to a few tens of meters above the ground. In some cases the logarithmic wind profile may be representative up to 100 meters above ground level, well beyond the top of the SBL. The logarithmic wind profile and attendant similarity assumptions can therefore apply in the layer of interest for the majority of diffusion testing at DPG.

The logarithmic wind profile (Equation 3.12) should be contrasted with the empirical power law wind profile,

13

Because of the influence of roughness length on the wind profile, test sites for turbulence measurements must be carefully chosen. Variations in roughness with wind fetch greatly complicate interpretation of turbulence measurements. Also, introduction of man-made obstacles should be kept to a minimum at turbulence measurement sites. For sites with trees, large bushes, or similar impediments to flow, a correction factor, displacement height (d), must be introduced. Displacement height is a function of the height and the spacing of the flow impediments. Like z_0, d is a characteristic of flow at a specific site, and may suffer from aerodynamic effects similar to z_0 in strong winds. The least complicated test sites for turbulence measurements contain no obstacles to cause a requirement for d. At DPG, bushes are widely spaced and generally less than half a meter tall. Therefore, d is considered inconsequential because of the general absence of large or densely packed obstacles to the flow. The full form of the logarithmic wind profile equation for an adiabatic atmosphere is given by Equation 3.10, with $u_{(z)}$ representing a mean wind at height z (valid for $z > (d+z_0)$).

$$\overline{u}_{(z)} = (u_*/k) \ln((z-d-z_0)/z_0) \qquad (3.10)$$

At well chosen test sites, z_0 and d are small enough to be neglected in the numerator of Equation 3.10.

To this point, the effects of stability on the wind profile have not been discussed. For near-neutral conditions, a plot of wind speed versus height is nearly a straight line on a log-linear plot, as in Figure 3.1. However, the wind profiles show significant departures from linearity for diabatic conditions. During unstable conditions, the wind profile is expected to increase more slowly than in the neutral case and, in stable conditions, the wind profile increases more rapidly than in the neutral case (Figure 3.1). To account for departures from linearity, a new variable, ϕ_m, the dimensionless wind shear, is introduced to Equation 3.9 so that

$$\partial \overline{u}/\partial z = u_* \phi_m/kz, \qquad (3.11)$$

and a diabatic influence function (ψ) derived as a function of ϕ_m by Paulson (1970) is introduced to the logarithmic wind profile, as shown in Equation 3.12.

$$\overline{u}_{(z)} = (u_*/k) \ln((z/z_0)-\psi) \qquad (3.12)$$

Equation 3.13 presents the functional relationship of ψ to ϕ_m.

$$\psi = 2 \ln((1 + \phi_m^{-1})/2) + \ln((1+ \phi_m^{-2})/2) -2\tan^{-1}\phi_m^{-1} + \pi/2 \qquad (3.13)$$

12

$$(u_2 - u_1)/u_* = \ln(z_2/z_1)/k, \qquad (3.8)$$

where k is an empirical constant known as von Karman's constant. Wind profile studies showing a linear relationship between u and ln z under adiabatic conditions tend to confirm the validity of Equation 3.8. The derivative of Equation 3.8 over an infinitesimal height yields the basis of a fundamental flux-gradient relationship, given in Equation 3.9.

$$\partial \overline{u}/\partial z = u_*/kz \qquad (3.9)$$

If z_1 in Equation 3.8 is chosen sufficiently close to the ground, u_1 is at the top of the viscous sublayer and is free of Reynolds stress momentum transfers from above. This sublayer height is determined by the dynamic roughness of the underlying surface. The dynamic roughness height (z_0), according to Monin and Obukhov (1954), defines the characteristic scale of the underlying surface's micro nonuniformities. The magnitude of z_0 is determined by the properties of the underlying surface alone and should be independent of wind speed. In practice, z_0 changes somewhat as a function of wind speed because as wind speed increases, plants or other roughness elements may assume more aerodynamically efficient shapes to reduce drag.

Determination of z_0 for a given site is done experimentally, with careful measurements near the surface by using fast response instruments, such as hot wire anemometers. For very flat surfaces, z_0 can be less than one centimeter. Conversely, z_0 can approach 1 meter in built-up urban areas. For near neutral wind profiles, z_0 may be obtained at the intersection of the linear wind profile at u = 0 on a plot of u versus ln z (Figure 3.1). Estimates of z_0 are obtained from the averages of repeated measurements using this procedure. Rough estimates of z_0 can also be obtained from the general characteristics of the site, as demonstrated by Hogstrom and Hogstrom (1978). Analysis of wind fields at DPG yield z_0 values ranging from 2 to 4 cm.
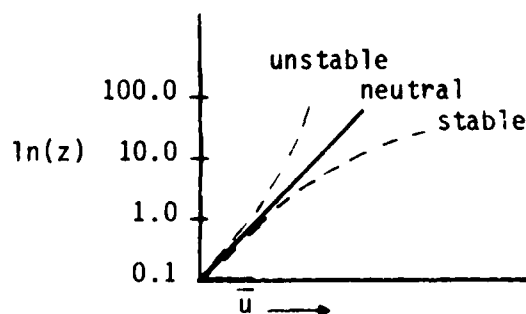

Figure 3.1. Wind Speed Versus Height (logarithmic scale).

11

The SBL, extending from a few centimeters to several tens of meters above the
surface, is of great interest in turbulence and diffusion studies because this
is the layer in which most human activities occur. Within the SBL the ratio
τ/ρ is nearly constant. This ratio has units of $m^2 sec^{-2}$, the square root of
which yields units of velocity. Consequently, the square root of τ/ρ is de-
fined as the friction velocity (u_*). In the SBL,

$$-\overline{u'w'} = \tau/\rho \equiv u_*^2. \tag{3.3}$$

Friction velocity is the characteristic velocity within the SBL. It accounts
for the effects of large scale pressure gradients and surface roughness
effects on SBL winds (see Tennekes, 1982). Friction velocity is used to form
dimensionless ratios with other SBL winds. The nondimensional SBL winds can
then be conveniently described as a function of height, surface roughness, and
stability.

Monin and Obukhov (1954) used similarity between laboratory flow and flow
within the SBL to obtain a logarithmic form of the wind profile. Within the
SBL, the mean wind speed difference at two heights is related to the ratio of
the heights as expressed in Equation 3.4,

$$(u_2-u_1)/u_* = f(z_2/z_1) \tag{3.4}$$

where f represents a function. To find the nature of f, three wind speed and
height combinations were chosen such that $z_3 > z_2 > z_1$ and $u_3 > u_2 > u_1$.

Because

$$u_3 - u_1 = (u_3 - u_2) + (u_2 - u_1) \tag{3.5}$$

and

$$z_3/z_1 = (z_3/z_2) \cdot (z_2/z_1), \tag{3.6}$$

the functional form that satisfies Equations 3.5 and 3.6 is the logarithmic
equality presented in generalized form using Equation 3.7.

$$\ln(\xi_3/\xi_2) \cdot \ln(\xi_2/\xi_1) = \ln(\xi_3/\xi_1) = \ln\xi_3 - \ln\xi_1 =$$
$$(\ln\xi_3 - \ln\xi_2) + (\ln\xi_2 - \ln\xi_1) \tag{3.7}$$

Therefore, the required functional relationship between the nondimensionalized
wind of Equation 3.4 and the height ratio is,

10

L. F. Richardson is said to have stated it as follows:

> Great whorls have little whorls
> That feed on their velocity...
> And the little whorls have lesser whorls,
> And so on to viscosity.

3. THE LOGARITHMIC AND POWER LAW WIND PROFILES:

Two empirical equation forms, the logarithmic and power law profiles, describe the change in wind speed with height. The logarithmic profile originated with laboratory fluid flow measurements and has become part of the system of equations used for similarity theory descriptions of the turbulent atmosphere. Power law profiles came from attempts to fit vertical wind speed measurements with a simple exponential equation. The simpler power law forms are more mathematically tractable for use with diffusion equations than are logarithmic profiles.

To overcome the impasse presented by intractable Navier-Stokes equations, fluid dynamicists used laboratory experiments for engineering solutions to fluid dynamics problems. A number of very useful semi-empirical relationships were developed from these experiments. One is the Reynolds Number (RE), a dimensionless ratio of accelerations to viscous stress gradients. When RE is large, flow is considered to be fully turbulent regardless of the scale of the experiment. With a large RE, the principle of dynamic similitude can be used to relate laboratory findings to turbulent processes in the atmosphere. Dynamic similitude considerations led to the application of logarithmic fluid velocity profiles observed in the laboratory to wind flow in the friction layer near the ground.

Several unique flow layers have been found in laboratory flow simulations. In pipe flow, there is a thin layer (the viscous sublayer) close to the wall where the influence of viscosity is great and the viscous shear stress $(\mu\ \partial u/\partial z)$ is much larger than the Reynolds shear stresses. The viscous sublayer is often called the laminar sublayer due to absence of Reynolds stress. Stress at the wall (τ_0) is given by Equation 3.1, where $\bar{u}$ is now defined as a mean wind along the direction of flow.

$$\tau_0 = \mu\ \partial\bar{u}/\partial z \qquad (3.1)$$

Outside the viscous sublayer in pipe flow, stress remains constant at its wall value $(\tau \simeq \tau_0)$, but Reynolds stresses are predominant and viscous effects are small. Soviet scientists Monin and Obukhov (1954) noted the similarity of this pipe flow phenomenon to observed flows in the atmosphere. They defined the atmospheric constant stress layer, also known as the surface boundary layer (SBL), as a layer several tens of meters in depth in which

$$\tau \simeq \tau_0 = -\rho\overline{u'w'} \simeq \text{constant.} \qquad (3.2)$$

When winds are divided into mean ($\bar{u}$) and fluctuating (u') components, the assumption is made that the sampling time is sufficiently short so variations in the mean motion are negligible, and sufficiently long so that the average value of u' approaches zero. In other words, a "spectral gap" is assumed to exist between the mean and turbulent components of flow. 'n practice, this condition can be approached over uniform terrain in the atmospheric surface layer with sampling times of 10 to 60 minutes, assuming that the wind field is not perturbed by transient mesoscale features. Under the assumption that a spectral gap exists, the flow is statistically stationary, i.e., turbulence statistics of the flow do not change with time and may be adequately represented by time averages obtained from equipment mounted at fixed locations past which the fluid travels.

To illustrate energy transfer from mean to turbulent flow, consider an average size eddy subjected to finite positive $\partial w/\partial z$ in a fluctuating wind field containing eddies larger and smaller than the eddy in question. If eddy volume remains constant, stretching of the eddy in the z direction by the motions of larger eddies will be accompanied by contraction along the horizontal axis. Conservation of angular momentum requires the product of vorticity and radius to remain constant in the absence of viscous dissipation. For example, conservation of angular momentum is the cause of the increase in spin of an ice skater who brings his/her arms in close to his/her body. Consequently, the response of an eddy to $\partial w/\partial z$ stretching is an increase in the horizontal component of eddy vorticity as the horizontal dimensions of the eddy decrease. Vertical stretching therefore causes an anomaly in the horizontal wind field. As the larger eddies stretch the sample eddy, smaller eddies are being stretched by the sample eddy, diluting its vorticity. The length scale of eddies decreases with stretching and mixing at each stage, establishing a cascade of energy to smaller eddy sizes.

As energy progressively cascades to smaller length scales, there is an increasing tendency for equipartition of eddy energy along each axis. The condition of local homogeneity is achieved at the scale where the eddy statistical properties depend only on spatial separations and time differences. Isotropy occurs as the eddy properties become independent of axes orientation. The eddy size at which isotropy occurs is limited by height above the ground. The probability that larger eddy sizes will exhibit isotropy increases with height above the surface. For measurements at a given height, the largest eddy size for which isotropy occurs represents the beginning of the inertial subrange. The spectrum of eddy sizes in the inertial subrange is a function of the rate of turbulent energy dissipation per unit mass (ϵ). At progressively smaller eddy sizes, the inertial subrange merges into the viscous subrange, where the eddy size spectrum is a function of μ/ρ and ϵ. At the lower end of the viscous subrange, eddy energy is converted to the kinetic energy of molecular motion (heat). Thus the nonlinear Reynolds stress terms of the Navier-Stokes equations extract energy from the mean flow and cascade it down the spectrum of eddy sizes. The viscous term acts as a sink at the lower end of the spectrum.

Following the above arguments, Bradshaw (1971) defines turbulence as a three-dimensional time-dependent motion in which vortex stretching causes velocity fluctuations to spread to all wavelengths between a minimum determined by viscous forces and a maximum determined by the boundary conditions of the flow.

A more useful form of Equation 2.10 is obtained by assuming nondivergence for the fluctuating components,

$$\partial \overline{u}' / \partial x + \partial \overline{v}' / \partial y + \partial \overline{w}' / \partial z = 0, \qquad (2.11)$$

Multiplying Equation 2.11 by $\overline{u}'$, and recognizing that

$$\partial(\overline{u'u'})/\partial x + \partial(\overline{u'v'})/\partial y + \partial(\overline{u'w'})/\partial z = \overline{u}' \; \partial \overline{u}'/\partial x + \overline{u} \; \partial \overline{v}'/\partial y +$$
$$\overline{u}' \; \partial \overline{w}'/\partial z + \overline{u}' \; \partial \overline{u}'/\partial x + \overline{v}' \; \partial \overline{u}'/\partial y + \overline{w}' \; \partial \overline{u}'/\partial z, \qquad (2.12)$$

the variance and covariance terms on the left side of Equation 2.12 can be substituted into the fluctuating part of Equation 2.10. This produces the mean equation of motion in an atmosphere containing mean and fluctuating components as shown in Equation 2.13.

$$d\overline{u}/dt = (-1/\rho) \partial P/\partial x + f_c + (\mu/\rho) \partial^2 \overline{u}/\partial z^2 + (1/\rho) \; \partial(-\rho\overline{u'u'})/\partial x +$$
$$(1/\rho) \; \partial(-\rho\overline{u'v'})/\partial y + (1/\rho) \; \partial(-\rho\overline{u'w'})/\partial z \qquad (2.13)$$

The mean terms in Equation 2.13 are similar to those in Equation 2.3, with the major difference being the addition of mean fluctuating component products. The additional terms formed from the variances and covariances of fluctuating wind components are known as Reynolds stresses. In the atmosphere, Reynolds stresses are larger than the viscous terms of the Navier-Stokes equations except very near the surface. The vertical terms containing $-\rho\overline{u'w'}$ are of greatest interest because the rate of change in stress in the x and y directions is usually assumed to be small [i.e., $\partial(\overline{u'u'})/\partial x$, $\partial(\overline{u'v'})/\partial y$ approach zero]. Shear stress is defined in Equation 2.14 for the $\overline{u'w'}$ covariance term.

$$\tau_{zx} = -\rho\overline{u'w'} = -F_m \qquad (2.14)$$

The $\overline{u'w'}$ of Equation 2.14 must be represented by $((\overline{u'w'})^2 + (\overline{v'w}^2))^{\frac{1}{2}}$ in the atmoshere. Equation 2.14 describes the mean transport of u' per unit time through a horizontal plane, which is a the vertical component of momentum flux (F_m) due to Reynolds stress. Comparison of Equations 2.1 and 2.14 shows that a gradient imposed on a flow containing mean and fluctuating components will cause a momentum flux to develop. Flux-gradient relationships are developed further in Section 6.

In Figure 2.3.a, $\partial u/\partial x + \partial v/\partial y$ is negative, and $\partial w/\partial z$ must be equal and of opposite sign if the total velocity vector remains nondivergent. This condition, where the horizontal component ($\nabla_h \cdot \vec{V}$) is negative, is known as convergence. Figure 2.3.b demonstrates the opposite effect for divergence ($\nabla_h \cdot \vec{V}$ positive and $\partial w/\partial z$ negative). In addition to convergence/divergence, a fluid cross can display rotation about the origin, or vorticity (Figure 2.4).
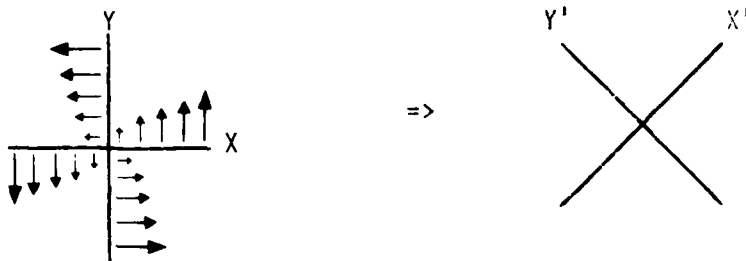
Figure 2.4. Vorticity ($\partial v/\partial X - \partial u/\partial y$).

The divergence and vorticity concepts introduced above are used with the equations of motion to describe the action of turbulence. First, however, additional stress terms caused by atmospheric eddy motions must be introduced. Consider an instantaneous wind field (u) divided into its mean ($\bar{u}$) and fluctuating (u') components such that the time average of individual fluctuating components is zero (u' = 0), but the products u'u', u'v', etc. can be nonzero. Then, the x component of mass inflow, or momentum flux, through area $\Delta y \Delta z$ in Figure 2.2 is

$$u(\rho u \Delta y \Delta z) = \rho u^2 \Delta y \Delta z = \rho(\bar{u} + u')^2 \Delta y \Delta z = \rho(\bar{u}^2 + 2\overline{uu'} + u'^2) \Delta y \Delta z \qquad (2.9)$$

The mixed products (such as $\overline{uu'}$) average to zero, but the average of products of the fluctuating terms ($\overline{u'w'}$, etc.) are nonzero so long as there is some degree of correlation between the fluctuating components. These nonzero products must be considered in the equations of mean motion.

To show the contribution of fluctuating variance and covariance terms to the mean Navier-Stokes equations, divide the total derivative du/dt (from Equation 2.3) into its local ($\partial u/\partial t$) and advective ($\vec{V} \cdot \nabla u$) components and expand it into mean (u) and average fluctuating ($\bar{u}'$) components. The nonzero products are

$$du/dt = \partial\bar{u}/\partial t + \bar{u}\,\partial\bar{u}/\partial x + \bar{v}\,\partial\bar{u}/\partial y + \bar{w}\,\partial\bar{u}/\partial z \qquad (2.10)$$
$$+ u'\,\partial u'/\partial x + v'\,\partial u'/\partial y + w'\,\partial u'/\partial z$$

Because

$$-\partial\rho/\partial t = \nabla\cdot\rho\vec{V} = \vec{V}\cdot\nabla\rho + \rho\nabla\cdot\vec{V}, \tag{2.6}$$

and assuming horizontal changes in density are small (ρ constant in space and time) over small distances in the surface boundary layer (SBL), it is reasonable to assume that the fluid is homogeneous and incompressible. Then,

$$-\partial\rho/\partial t = 0, \quad \vec{V}\cdot\nabla\rho = 0, \quad \rho\nabla\cdot\vec{V} = 0. \tag{2.7}$$

Of the equations represented in Equation 2.7, the divergence equation ($\rho\nabla\cdot\vec{V} = 0$) is the one of interest. Equation 2.8 is the divergence equation for a non-divergent velocity vector.

$$\nabla\cdot\vec{V} = \partial u/\partial x + \partial v/\partial y + \partial w/\partial z = 0 \tag{2.8}$$

Eddy motions in the atmosphere are conveniently described with the aid of a "fluid cross" which defines the area occupied by a slice through a hypothetical eddy. A two-dimensional representation of the hypothetical eddy undergoing horizontal convergence and divergence is shown in Figures 2.3.a and b. Arrows in the figures represent velocity components along each axis, depicting $\partial u/\partial x$ and $\partial v/\partial y$.

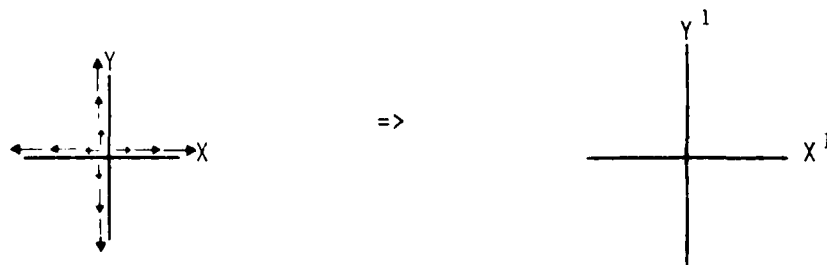Figure 2.3.a. Convergence ($\partial u/\partial x + \partial v/\partial y$ negative, horizontal area decreases)

Figure 2.3.b. Divergence ($\partial u/\partial x + \partial v/\partial y$ positive, horizontal area increases)

5

For practical purposes, K is usually specified in diffusion equations for an inert passive scalar of neutral buoyancy. Other adjustments are then made within models to account for departures from this condition.

With the foregoing discussion of K in mind, Equation 4.6 can be configured for application to specific types of diffusion problems. If turbulence is assumed to be isotropic, i.e., negligible variation in diffusivity with respect to spatial orientation, then

$$K_x = K_y = K_z = K \tag{4.13}$$

When Equation 4.13 is satisfied and K is constant, simple or Fickian diffusion occurs. For the limiting condition where $\vec{V}$ equals zero and Equation 4.13 holds, Equation 4.6 reduces to the Laplacian (∇^2) of concentration multiplied by K

$$\partial\bar{\chi}/\partial t = K(\partial^2\bar{\chi}/\partial x^2 + \partial^2\bar{\chi}/\partial y^2 + \partial^2\bar{\chi}/\partial z^2) = K\nabla^2\bar{\chi}. \tag{4.14}$$

Equation 4.14 applies to instantaneous point source releases such as a puff formed by the air burst of a smoke munition under calm wind conditions.

For the more general condition where $\vec{V} \neq 0.$, the axis of plume travel is chosen so that it is along the axis of the mean horizontal wind. With the condition that the mean vector wind is finite only along the x axis, the vector wind equation is reduced to Equation 4.15

$$\vec{V} = \vec{i}u; \text{ with } \vec{j}v, \vec{k}w = 0, \tag{4.15}$$

where $\vec{i}$, $\vec{j}$, $\vec{k}$ are unit vectors in the x, y, and z directions.

Then Equation 4.6 becomes

$$(\partial\bar{\chi}/\partial t + u\,\partial\bar{\chi}/\partial x) = \partial(K_x\,\partial\bar{\chi}/\partial x)/\partial x + \partial(K_y\,\partial\bar{\chi}/\partial y)/\partial y + \partial(K_z\,\partial\bar{\chi}/\partial z)/\partial z. \tag{4.16}$$

If a further assumption is made that steady state conditions exist, the first term on the left of Equation 4.16 $(\partial\bar{\chi}/\partial t)$ is negligible. For a continuous point source (such as a plume from a smoke stack), the rate of change in $\partial\bar{\chi}/\partial x$ along the x axis is negligible and the term $\partial^2\bar{\chi}/\partial x^2$ is zero. A further simplification of the diffusion equation is obtained if a continuously emitting infinite line source is oriented normal to the mean wind direction. Then, $\partial\bar{\chi}/\partial y$ is also zero and Equation 4.16 is reduced to

$$\bar{u}\,\partial\bar{\chi}/\partial x = K_z\,\partial^2\bar{\chi}/\partial z^2 \tag{4.17}$$

19

In reality, the horizontal wind direction is rarely steady, source emissions vary with time, and line sources are never infinite. When using a model that requires these assumptions, it is prudent to have information on the degree of departure from the idealized conditions described in the preceeding paragraphs. The information required involves resolution of the motion fields that the plume is subjected to and knowledge of the plume's source geometry and temporal variability. The problem is further complicated by the fact that although the plume is subjected to turbulence as it is carried along by the wind (Lagrangian coordinate system), wind and turbulence measurements are usually made from fixed points (Eulerian coordinate system). Point measurement devices on a single tower are rarely adequate for providing the necessary field measurements, although several measurement positions along the path of plume travel would help provide the required information. These measurements, integrated with the mesoscale wind field measurements in a well defined synoptic pattern, are required to obtain an adequate description of atmospheric motion fields.

In addition to difficulties with K-theory expressions, modelers are faced with the problem of cloud centroid motions. Laboratory measurements (see, for example, Willis and Deardorff, 1976) indicate that cloud centroids often do not remain at the height of release. Caughey et al. (1983) verified this finding in their convective boundary layer (CBL) turbulence structure studies. Caughey et al. note that downdrafts cover more than half of the horizontal area in the CBL, the effect of which is a net descent of material released into the upper part of the CBL. For surface releases, the centroid can either ascend or move horizontally, since it cannot penetrate the ground. In convection, updrafts lift the centroid off the ground, while downdrafts can only cause horizontal spreading. The net result is that cloud centroids ascend from the surface or descend from aloft until they reach approximately half the boundary layer depth. Consequently, the condition $w = 0$. (Equation 4.15) does not guarantee that a CBL cloud centroid will remain at its release height. Measurements of divergence field changes, vertical wind profiles, and atmospheric stability are indicators of the degree of convective activity and the consequent centroid height changes. For diffusion tests, downwind sampling to monitor the cloud centroid movements is prudent. Failure to identify changes in the vertical position of the cloud centroid is a major cause of uncertainty in diffusion cloud characterization.

Analytic solutions for χ in the above equations follow from mathematical procedures describing molecular conduction of heat in a solid, as suggested by Roberts (1923). Pasquill and Smith (1983) note that the solutions are most readily obtained by adopting power law forms of the K and wind profiles,

$$K_{z(z)} = K_1 \left(\frac{z}{z_1}\right)^n, \qquad u_{(z)} = u_1 \left(\frac{z}{z_1}\right)^m \qquad (4.18)$$

The most widely used analytic solutions for diffusion problems are the Gaussian diffusion equations. These are obtained using the following assumptions:

a. Exponents $m = n = 0$ in Equation 4.18. The result is that K and u are taken to be constant with height.

b. Travel distance downwind of the source equals ut, where u is a transport wind and t is travel time.

c. A relationship exists between K, t, and the standard deviation of plume material distribution (σ) so that

$$\sigma = \sqrt{2Kt} \qquad (4.19)$$

With the above assumptions, it is possible to take advantage of the fact that the area under the Gaussian (normal) curve is unity. Consider the z component of a diffusing cloud moving downwind with the x axis defined along the cloud centroid. From integral tables,

$$\int_{-\infty}^{\infty} EXP\ (-z^2/2\,\sigma_z^2) = \sqrt{2\pi}\ \sigma_z \qquad (4.20)$$

Then,

$$\int_{-\infty}^{\infty} 1/(\sqrt{2\pi}\ \sigma_z)\ EXP(-z^2/2\sigma_z^2) = 1.0 \qquad (4.21)$$

Similar relations hold for the x and y components. Therefore, the distribution of cloud material at varying distances downwind from a source can be described as a function of cloud sigmas, providing a concise statement of continuity for use in diffusion models.

Given the above assumptions, Gaussian diffusion equations are obtained for the appropriate sets of boundary conditions (Pasquill and Smith, 1983):

a. Instantaneous point source. The initial boundary conditions are:

$$\overline{\chi} \to 0 \text{ as } x,z \to \infty \qquad (4.22)$$

$$\overline{\chi} \to \infty \text{ as } x,z \to 0. \qquad (4.23)$$

$$K_z\, \partial\overline{\chi}/\partial z \to 0. \text{ as } z \to 0., x>0. \qquad (4.24)$$

For an instantaneous release in zero wind, the source strength (Q grams) is the total volume integral of concentration, i.e.,

$$\iiint \overline{\chi} \; \Delta x \Delta y \Delta z = Q. \tag{4.25}$$

The solution for instantaneous point source Fickian diffusion from Equation 4.14 is:

$$\overline{\chi} = (Q/(2^3(2\pi)^{3/2}\sigma_x\sigma_y\sigma_z)) \; EXP \; [- \; (x^2/2\sigma_x^2 + y^2/2\sigma_y^2 + z^2/2\sigma_z^2)] \tag{4.26}$$

b. Continuous point source. For a continuous release from a point source, where Q is expressed in units of grams/second, the additional boundary conditions required to obtain a solution from Equation 4.16 are:

$$\partial\overline{\chi}/\partial t = 0., \; \partial^2\overline{\chi}/\partial x^2 = 0. \tag{4.27}$$

and

$$\iint \overline{\chi} \overline{u} \Delta y \Delta z = Q \tag{4.28}$$

The solution is:

$$\overline{\chi} = (Q/(2\pi\sigma_y\sigma_z \overline{\overline{u}})) \; EXP \; [- \; (y^2/2\sigma_y^2 + z^2/2\sigma_z^2)] \tag{4.29}$$

c. Continuous infinite crosswind line source. The additional boundary condition is:

$$\partial\overline{\chi}/\partial y = 0. \tag{4.30}$$

For the continuous release from a line source, the source strength Q (grams/meter second) is equivalent to the expression

$$\int \overline{\chi} \overline{\overline{u}} \Delta z = Q \tag{4.31}$$

22

The solution to an infinite line source obtained from Equation 4.17 is

$$\overline{\chi} = (Q/(\sqrt{2\pi}\ \sigma_z \overline{\overline{u}}))\ \text{EXP}\ [-\ (z^2/2\sigma_z^2)] \tag{4.32}$$

The three solutions given above do not include provisions for calculation of concentrations at points not at the cloud centroid or for reflection of the cloud from an impervious surface. See Sutton (1953) or Pasquill and Smith (1983) for further discussion of these provisions.

The assumptions of constant u and K are very restrictive because both vary significantly with height. To compensate for the variation of u with height, diffusion models make use of a "transport wind", $\overline{\overline{u}}$. The transport wind is a mean wind obtained by averaging over the depth of the plume and for plume travel time. This wind averaging over space and time should be representative of the rate of the diffusing cloud's downwind travel. A number of procedures exist for estimating $\overline{\overline{u}}$. Cramer et al. (1972) offer an algorithm for $\overline{\overline{u}}$ based on the 1 or 2 meter wind speed. For downwind hazard distance calculations at DPG, the first 1/2- or 1-minute elevation angle readings from 10-grams ceiling balloons are frequently used to estimate $\overline{\overline{u}}$. Continuous time and space averaged vertical wind profiles available from modern remote sensing devices should permit more satisfactory $\overline{\overline{u}}$ estimates.

To compensate for assuming a constant K and using the $\sigma = \sqrt{2Kt}$ relation, much effort is expended in attempts to describe σ as a function of atmospheric stability parameters, measured turbulence, and downwind travel distance. The simplest approaches are those developed by Pasquill (1961), with σ varying as a function of information obtainable from general weather observations (sun angle, cloud cover, and wind speed). The Pasquill procedure, further developed by Turner (1964) is currently used as a stability category input for DPG hazard calculations. An updated and improved form of this procedure, based on net radiation measurement, is described in Myirski (1983). To avoid the limitations of the stability category approach, measured or calculated values of turbulence can be used in sigma calculations for the diffusion equations. Sigma e, for example, is derived as a function of stability parameter z/L in Section 7. Sigma z can then be calculated as $\sigma_e \times f(x)$.

K-theory simplifications leading to the Gaussian diffusion equations permit concise solutions for diffusion problems. Given a source strength, release height, configuration and duration, cloud dimensions in sigmas, and a transport wind, concentrations downwind from a source can be readily calculated. However, the performance of a Gaussian model is limited and expectations that solutions will fit a given set of measured concentrations cannot be too high (Smith, 1984). At best, many replications of measurements made during similar atmospheric conditions will, on the average, approach the Gaussian calculated value.

Some of the limitations of Gaussian models are overcome through the application of similarity concepts to diffusion. Similarity models have been based on the hypothesis that the Eulerian properties which characterize the SBL can be applied to the Lagrangian motions of particles within the SBL. Model

developments by Horst (1979) and Nieuwstadt and van Ulden (1978) show promise in overcoming some Gaussian model limitations. However, similarity theory has not successfully treated extremely stable nocturnal situations common at DPG. Even with this limitation, future model development at DPG should include consideration of similarity applications to diffusion. New K-theory treatments by Wyngaard and Brost (1984) and Fiedler (1984) should also be investigated for applications at DPG.

5. KINETIC ENERGY AND THE RICHARDSON NUMBERS

Atmospheric stability is related to turbulence through the turbulent kinetic energy (TKE) equation. First attempts to relate turbulence to stability criteria were made by Mr. L. F. Richardson in the 1920s (Richardson, 1925). These dimensionless stability criteria came to be known as Richardson Numbers. A complete derivation of a criterion of turbulence for the atmosphere was made by Calder (1949) using the TKE equation. Calder achieved the derivation by defining turbulent kinetic energy as the difference between the instantaneous and mean kinetic energy equations, with particular attention to Reynolds stress terms. Derivation of Richardson numbers from the TKE equation in this section follows Calder's procedure, but uses simplified notation.

The instantaneous vector equation of motion is

$$\rho d\vec{V}/dt + \rho \vec{f}_c = \vec{g}\rho - \nabla P + \mu\nabla^2\vec{V} \tag{5.1}$$

where $d\vec{V}/dt$ is a total derivative of the vector wind while $\vec{f}_c$, $\vec{g}$, $\nabla P/\rho$, and $\mu\nabla^2\vec{V}/\rho$ represent forces per unit mass due to the Coriolis effect, gravity, pressure gradient, and viscous dissipation. The dot product of Equation 5.1 with the velocity vector $\vec{V}$ produces the kinetic energy equation of instantaneous motion

$$\tfrac{1}{2}\rho dV^2/dt = -wg\rho - \vec{V}\cdot\nabla P + \vec{V}\cdot\mu\nabla^2\vec{V} \tag{5.2}$$

Note that the Coriolis term drops out of the equation because

$$\vec{V}\cdot\vec{f}_c = \vec{V}\cdot 2\Omega \times \vec{V} = 0. \tag{5.3}$$

Also, because the force of gravity only operates in the z direction, the dot product of the velocity vector with this term reduces to the scalar $wg\rho$.

On the left side of Equation 5.2 the dotted velocity vectors have been reduced to the scalar V^2 where

24

$$V^2 = (u^2 + v^2 + w^2).\tag{5.4}$$

The total differential $\rho dV^2/dt$ expanded into its component parts is

$$\rho dV^2/dt = \rho \partial V^2/\partial t + \rho \vec{V}\cdot\vec{\nabla}V^2\tag{5.5}$$

In the next series of steps, the total differential is replaced with its components in the desired form. The continuity equation is introduced as a product with V^2

$$V^2\partial\rho/\partial t + V^2\partial(\rho u)\partial x + V^2\partial(\rho v)/\partial y + V^2\partial(\rho w)/\partial z = 0.\tag{5.6}$$

Because

$$V^2\partial\rho/\partial t = \partial(V^2\rho)\partial t - \rho\partial V^2/\partial t\tag{5.7}$$

and using similar relationships for other components of Equation 5.6, the total differential in Equation 5.2 can be replaced by

$$\tfrac{1}{2}[\partial(\rho V^2)/\partial t + \partial(\rho V^2 u)/\partial x + \partial(\rho V^2 v)/\partial y + \partial(\rho V^2 w)/\partial z]$$
$$= -wg\rho - \vec{V}\cdot\nabla p + \vec{V}\cdot\mu\nabla^2\vec{V}\tag{5.8}$$

The left side of Equation 5.8 can be written in tensor notation following Calder (1949), yielding

$$[\partial(\rho u_i^2)/\partial t + \partial(\rho u_i^2 u_k)/\partial x_k] = -wg\rho - \vec{V}\cdot\nabla p + \vec{V}\cdot\mu\nabla^2\vec{V}\tag{5.9}$$

The instantaneous equation of motion is next separated into mean (ρ, v) and turbulent (ρ', v') components. Because the average of each turbulent component is zero, the average value of terms containing a single turbulent component is zero. However, terms containing multiple turbulent components ($\rho'u'$, $u'w'$, etc.) have nonzero averages. Using these rules, ρu_i^2 from the left side of Equation 5.9 becomes

$$\overline{\rho u_i}^2 = (\overline{\rho} + \overline{\rho}')(\overline{u_i}^2 + 2\overline{u_i}\overline{u_i'} + \overline{u_i'}^2) = \overline{\rho u_i}^2 + \overline{\rho u_i'}^2 + 2\overline{\rho'}\overline{u_i}\overline{u_i'} + \overline{\rho'}\overline{u_i'}^2\tag{5.10}$$

The terms in Equation 5.10 containing $\bar{\rho}'$ are 3 or 4 orders of magnitude smaller than terms containing $\bar{\rho}$ and are usually neglected. The second term on the left side of equation 5.9 is treated in a similar manner. The result (neglecting terms with $\bar{\rho}'$) is

$$\overline{\rho u_i^2 u_k} = \bar{\rho}(\overline{u_i}^2 \overline{u_k} + \overline{u_i'^2}\,\overline{u_k} + 2\overline{u_i}\,\overline{u_i'u'}_k + \overline{u_i'^2 u_k'}) \tag{5.11}$$

On the right side of Equation 5.9, $wg\rho$ is expanded to

$$wg\rho = \overline{w}g\bar{\rho} + w'g\rho' \tag{5.12}$$

In this case $\overline{w'g\bar{\rho}'}$ is not neglected because it will be the remainder after the subtraction of two larger terms in Equation 5.19. The $\vec{V}\cdot\nabla P$ term is expanded to

$$\vec{V}\cdot\nabla P = \vec{V}\cdot\nabla\overline{P} + \vec{V}'\cdot\nabla\overline{P}' \tag{5.13}$$

The final term on the right side of Equation 5.9 is $\vec{V}\cdot\mu\nabla^2\vec{V}$. This is a dissipation term. With expansion into mean and turbulent components it becomes $\bar{\epsilon} + \bar{\epsilon}'$, where ϵ represents viscous dissipation into heat.

Gathering terms from Equations 5.10 to 5.13 the kinetic energy equation of instantaneous motion is given by

$$\tfrac{1}{2}\rho\, d(\overline{u_i}^2 + \overline{u_i'^2})/dt = \tfrac{1}{2}[\partial(\overline{\rho u_i}^2 + \overline{\rho u_i'^2})/\partial t + \partial(\bar{\rho}(\overline{u_i}^2\overline{u_k} + \overline{u_i'^2}\,\overline{u_k} +$$
$$2\overline{u_i}\,\overline{u_i'u_k'} + \overline{u_i'^2 u_k'}))/\partial x_k] = -\overline{w}g\bar{\rho} - \overline{w'g\rho'} - \vec{V}\cdot\nabla P - \vec{V}'\cdot\nabla P' + \bar{\epsilon} + \bar{\epsilon}' \tag{5.14}$$

The vector equation of mean motion, where Equation 2.13 defines the u component, is used as the starting point to obtain the kinetic energy equation of mean motion. The major difference between the mean and instantaneous equations is the treatment of Reynolds stress terms. The Reynolds stress terms are represented in tensor notation as

$$-\overline{\rho u_i' u_k'} = \tau_{ik} \tag{5.15}$$

Following a development similar to the instantaneous equation given above, the kinetic energy equation of mean motion is

26

$$\tfrac{1}{2}\bar{\rho}d(\overline{u_i}^2)/dt = \tfrac{1}{2}[\partial(\overline{\rho u_i}^2)/\partial t + \partial(\overline{\rho(\overline{u_i}^2\overline{u_k})})/\partial x_k]$$

$$= -\overline{w g \rho} - \overline{\vec{V}}\cdot\overline{\nabla P} + \overline{\epsilon} + \overline{u_i}\,\partial\tau_{ik}/\partial x_k \tag{5.16}$$

Applying the rules of partial differentiation to the Reynolds stress components yields the expression

$$\overline{u_i}\,\partial\tau_{ik}/\partial x_k = \partial(\tau_{ik}\overline{u_i})/\partial x_k - \tau_{ik}\,\partial\overline{u_i}/\partial x_k \tag{5.17}$$

Reynolds stress components are also found in the kinetic energy equation of instantaneous motion. From Equation 5.14

$$\tfrac{1}{2}[\partial(2\overline{\rho u_i u_i' u_k'})]/\partial x_k = \partial(-\tau_{ik}\overline{u_i})/\partial x_k \tag{5.18}$$

Term by term subtraction of the kinetic energy equation of mean motion from Equation 5.14 for instantaneous motion produces Equation 5.19, the TKE equation.

$$\tfrac{1}{2}\bar{\rho}d(\overline{u_i'}^2)/dt = \tfrac{1}{2}[\partial(\overline{\rho u_i'}^2)/\partial t + \partial(\overline{\rho(\overline{u_i'}^2\overline{u_k} + \overline{u_i}^2\overline{u_k})})/\partial x_k]$$

$$= -\overline{w g \rho} - \overline{\vec{V}'}\cdot\overline{\nabla P} + \overline{\epsilon} + \tau_{ik}\,\partial\overline{u_i}/\partial x_k \tag{5.19}$$

The term w'gρ' is transformed into more useful form by recognizing from the equation of state that

$$P'/\bar{P} \simeq \rho'/\bar{\rho} + T'/\bar{T}. \tag{5.20}$$

Calder (1949) demonstrates that the ratio of pressure fluctuations to mean pressure is several orders of magnitude smaller than corresponding density and temperature ratios. Also, the ratios of temperatures and potential temperatures (θ) are nearly equivalent. The approximation

$$\rho'/\bar{\rho} \simeq -\,\theta'/\bar{\theta} \tag{5.21}$$

is used in the term $-\overline{w'g\bar{\rho}'}$ to produce

$$-\overline{w'g\rho'} = g\overline{\rho}\ \overline{w'\theta'}/\overline{\theta} \qquad (5.22)$$

The remaining terms of Equation 5.19 are simplified using the assumption of horizontal homogeneous flow along the direction of the x axis. For this condition, mean lateral ($\overline{v}$) and vertical ($\overline{w}$) motions are zero and the rate of change of the turbulent components in the horizontal plane is zero. Consequently, the term $\overline{u_i'^2\overline{u}_k}$, where

$$\overline{u}_k = \overline{w} = 0 \qquad (5.23)$$

is zero in Equation 5.19. The term $\frac{1}{2}\partial(\overline{\rho(\overline{u_i'^2\overline{u}_k'})})/\partial x_k$ is only nonzero for the z direction is shown in Equation 5.24

$$\frac{1}{2}\partial(\overline{\rho(\overline{u_i'^2\overline{u}_k'})})/\partial x_k = \frac{1}{2}\partial(\overline{\rho(\overline{u'^2\overline{w'}} + \overline{v'^2\overline{w'}} + \overline{w'^3})})/\partial z \qquad (5.24)$$

On the right side of Equation 5.19, $\overrightarrow{V'}\cdot\nabla\overline{P'}$ is reduced to $\overline{w'\partial\overline{P'}}/\partial z$ because $\partial\overline{P'}/\partial x$ and $\partial\overline{P'}/\partial y$ are negligible in horizontally homogeneous conditions. Similarly, $\tau_{ik}\partial u_i/\partial x_k$ becomes $-\rho\overline{u'w'}\partial\overline{u}/\partial z$ because $\overline{v}$ and $\overline{w}$ are zero.

Gathering terms from Equations 5.22 through 5.24, the mean TKE equation for horizontal homogeneous flow is thus

$$[\partial(\overline{\rho u_i'^2})/\partial t] = \frac{1}{2}[\partial(\overline{\rho(\overline{u'^2} + \overline{v'^2} + \overline{w'^2})})/\partial t = \partial(\overline{\rho E})/\partial t$$
$$= -\frac{1}{2}\partial(\overline{\rho(\overline{u'^2\overline{w'}} + \overline{v'^2\overline{w'}} + \overline{w'^3})})/\partial z + g\overline{\rho}\overline{w'\theta'}/\overline{\theta} - \overline{w'\partial\overline{P'}}/\partial z - \overline{\rho u'w'}\partial\overline{u}/\partial z - \overline{\varepsilon'}, \qquad (5.25)$$

where E represents turbulent kinetic energy. If a further assumption is made that turbulent conditions are stationary ($\partial\overline{\varepsilon}/\partial t$ and $\partial\overline{\rho}/\partial t$ are zero), the time-dependent terms are eliminated, leaving the TKE equation composed of a vertical energy flux divergence term, a buoyancy energy production term, a term which represents energy transfer due to the fluctuating gradients of static pressure, a shear energy production term, and viscous dissipation. The partial differentiation rule (as applied to Reynolds stress components in Equation 5.17) is applied to $\overline{\varepsilon'}$. Viscous dissipation then has two components, $\frac{1}{2}\mu\partial^2(\overline{u'^2\overline{v'}})/\partial x^2$ and $-\frac{1}{2}\mu(\overline{v'\partial^2\overline{u'}})/\partial x^2$ and comparable terms in the y and z directions. Calder (1949) identifies the first term as making a small contribution and drops the term from the equation. The second term represents the mean rate of dissipation per unit volume of turbulent energy into heat. The sign of $\overline{\varepsilon'}$ in Equation 5.25 was changed to reflect the sign of the second term.

The flux divergence and fluctuating pressure terms are not amenable to direct measurement. Consequently, they are often dropped from the equations. Studies by Wyngaard and Cote (1971) and Frenzen (1983) suggest that these terms are frequently significant. Frenzen concludes that these terms contribute to the TKE equation at the rate of one fourth of the sum of shear and buoyancy contributions for unstable conditions. Further field studies of these phenomena are required to clarify the role of these terms in the TKE budget.

The two production terms in the TKE equation of greatest interest are the buoyancy and shear production terms. The buoyancy production term can be positive or negative depending on the sign of the heat flux $\overline{w'\theta'}$. Vertical heat flux enters the TKE equation as the buoyant force per unit mass $(g/\overline{\theta})$ that acts on an eddy whose temperature and vertical velocity differ from the surroundings by θ' and w'. As the eddy travels over a vertical distance ℓ, it performs specific work proportional to $(g/\overline{\theta})\theta'\ell$ that enters directly into the vertical component of TKE. On the other hand, the shear production term is always positive in the presence of the stress induced by air movement over a rough survade. According to Calder (1949), it represents the transformation of mechanical energy present in the mean motion to the mechanical energy of turbulent motion. The shear term is large near the surface, where the gradients $\partial\overline{u}/\partial z$ are large, and tends to decrease with height in the SBL. Shear usually makes a larger contribution to the horizontal than the vertical component of TKE.

Richardson Numbers are formed from ratios of the buoyancy to shear production terms of the TKE equation. The flux Richardson Number is a dimensionless stability parameter defined as

$$R_f = (g/\overline{\theta})(\overline{w'\theta'})/[(\overline{u'w'})(\partial\overline{u}/\partial z)] \qquad (5.26)$$

R_f is usually not calculated from direct measurements because it is a combination of fluxes and gradients, which requires substantial amounts of instrumentation. A more commonly used form of Richardson Number is the gradient Richardson Number (Ri). Ri is found by using K-theory flux-gradient relationships (Equations 4.8 and 4.10) and assuming the K_m/K_h ratio to be unity.

$$Ri = (K_m/K_h)R_f = (g/\overline{\theta})(\partial\overline{\theta}/\partial z)/(\partial\overline{u}/\partial z)^2 \qquad (5.27)$$

Richardson Numbers are zero during adiabatic conditions when $\overline{w'\theta'}$ and $\partial\overline{\theta}/\partial z$ approach zero. For diabatic conditions with an upward heat flux (due to vertical motion and lapse of potential temperature with height in excess of the adiabatic lapse rate) Richardson Numbers assume negative values. The converse is true for a downward heat flux or inversion conditions.

The advantage of Ri as a stability parameter is that the gradients $(\partial\overline{\theta}/\partial z)$ and $(\partial\overline{u}/\partial z)$ can be calculated from wind and temperature profile data, but gradient calculations also have disadvantages. Gradients of wind and temperature

are small in relation to the absolute values of those variables. The adiabatic lapse rate is 0.01°C/m and measurements of that order of accuracy are necessary for accurate gradient calculations. Most temperature instrument accuracies do not exceed 0.1°C. Comparable accuracies with wind measurements are also required. The problem of making accurate calculations of Ri from wind gradient measurements is further complicated because the squared value of $(\partial \bar{u}/\partial z)$ in the denominator of Equation 5.27 magnifies errors.

Another complication with the use of Richardson Numbers arises because the gradients of wind and temperature near the surface are height dependent. Gradients computed from measurements made at the 0.5 to 4 m above ground level (AGL) will differ considerably from gradients computed from simultaneous measurements made at 2 and 8 m AGL. Therefore, Richardson Numbers vary with height, and the data from which Richardson Numbers are derived must be carefully specified when Richardson Numbers obtained from different data sets are compared. Also, the temperature and wind measurements used to obtain $\partial \bar{u}/\partial z$ and $\partial \bar{\theta}/\partial z$ in Equation 5.27 must be made over identical time and height intervals. Gradient measurements not obtained this way yield unique values of Richardson Numbers which are useless outside the data set from which they are computed. The Obukhov length stability parameter, described in Section 6, does not exhibit a dependence on measurement height and can be used in place of Ri.

If wind measurements are available at only one level, another form of Richardson Number, known as the bulk Richardson Number (BU), can be used.

$$BU = 100(g/\bar{\theta})(\partial\bar{\theta}/\partial z)(z^2/\bar{u}^2) \qquad (5.28)$$

While dimensionally correct, BU is totally empirical. Because the temperature gradient in the numerator is small compared to $\bar{u}^2$, BU tends to be small. Therefore, the calculated value of BU is usually multiplied by 100 for comparison with other stability parameters. In spite of its empirical origins, BU performs surprisingly well as a criterion for turbulence conditions in the stable atmosphere where Ri fails because of uncertainties in wind gradients.

Richardson Numbers are useful as stability parameters when the assumptions made during simplification of the TKE equation are not seriously violated. When flow is not horizontal or homogeneous, or when significant changes in the flow occur with time, discarded terms in the TKE equation become significant and simple stability parameter estimates fail to represent existing turbulence conditions. Therefore, stability parameters should be used with caution as criteria for turbulence during periods of rapid transition such as sunrise or sunset, or in the presence of transient mesoscale systems. The usefulness of stability parameters in complex terrain or near surface discontinuities is also open to question. As micrometeorological measurement capabilities improve, new stability parameters which include more TKE terms will be developed.

30

6. THE OBUKHOV LENGTH AND z/L.

Obukhov (1971) recognized the requirement for a more fundamental stability parameter than the gradient Richardson number. Assuming that conditions remain homogeneous in space and stationary in time, momentum (F_m) and heat fluxes (F_h) remain nearly constant within the SBL.

$$F_m = \overline{\rho' u' w'} = -\tau_0 = \text{constant} \qquad (6.1)$$

$$F_h = c_p \rho \, \overline{w' \theta'} = \text{constant} \qquad (6.2)$$

The c_p of Equation 6.2 represents specific heat at constant pressure. Obukhov observed that wind shear ($\partial \overline{u}/\partial z$), which is very large near the surface, decreases rapidly with height and reasoned that there is a height above the ground where the dynamic or shear stress contributions balance the buoyant contributions to turbulence. This height or length scale is the Obukhov length (L). Monin and Obukhov (1954) conclude that SBL turbulence can be described as a function of three parameters: ($g/\overline{\theta}$), u_*, and $\overline{w'\theta'}$. The Obukhov length is composed of a combination of these parameters representing the ratio of buoyancy to shear terms in the TKE equation, which is similar to the flux Richardson Number (Equation 5.26). With the aid of Equations 3.3 and 3.11, shear is described in terms of u_*. Then,

$$R_f = \frac{(g/\overline{\theta})\,(\overline{w'\theta'})}{(\overline{u'w'})(\partial \overline{u}/\partial z)} = \frac{(g/\overline{\theta})(\overline{w'\theta'})}{-u_*^2\,(u_* \phi_m/kz)} = \frac{z}{\phi_m}\,\frac{k(g/\overline{\theta})(\overline{w'\theta'})}{-u_*^3} = \frac{z}{\phi_m(-L)}. \qquad (6.3)$$

The sign of L is chosen so that L is negative for unstable thermal stratification. Hereafter in this report, the Obukhov length proceeded by a minus sign (-L) implies heat flux directed away from the surface, associated with a lapse of potential temperature. Because ($g/\overline{\theta}$), $\overline{w'\theta'}$, and u_* remain nearly constant with height in the SBL, the magnitude of -L changes little within the first few tens of meters of the atmosphere. This is in contrast to the Richardson Numbers that can vary as a function of height. The Obukhov length has units of meters. Therefore, the ratio z/L is dimensionless. Obukhov intended for the height above the surface where z/L = 1 to be the height where balance exists between the buoyant and shear contributions to turbulent kinetic energy, and defined -L as the height of the sublayer of dynamic turbulence. This balance is actually achieved at a smaller value of z/-L (see Section 7).

Because it depicts the relative contributions of buoyancy and shear to turbulence, z/-L functions as a dimensionless stability parameter. When the buoyant contribution is small, the magnitude of -L is large with respect to the height of the SBL and z/-L approaches zero. Turbulence for this neutral condition is mechanical, caused by the effects of roughness elements and

surface shear stress [In the early morning hours, as the sun is rising, the atmosphere passes briefly through this condition]. As the ground is heated, $w'\theta'$ becomes significant and buoyant forces make a contribution to turbulence. Monin and Yaglom (1971) found that buoyancy effects contributing to turbulence as $z/-L$ exceeds 0.03. With increasing $w'\theta'$ (or as z increases with $w'\theta'$ constant), buoyancy contributions increase until the point is reached where the contributions of buoyancy and shear forces to turbulence production are in balance. This occurs as $z/-L$ approaches 0.35. As $z/-L$ increases beyond 0.35, buoyancy becomes progressively more dominant until a state of windless convection is reached. Windless convection, characterized by intense surface heating with light and variable winds, is the condition where shear production is negligible ($u_* \rightarrow 0.0$). Windless convection is frequently observed during the middle of summer days at DPG.

To this point, the contribution of latent heat effects on stability have been neglected. Dyer and Hicks (1970) accounted for latent heat effects on L as in Equation 6.4,

$$-L = c_p \rho \overline{T} u_*^3 / kg(F_h + 0.07 F_l)$$ (6.4)

where F_h and F_l represent fluxes of sensible and latent heat. At its maximum, F_l is only 16 percent of F_h. If available from humidity flux measurements, the F_l factor should be considered. At DPG, omission of F_l would generally result in a negligible error.

There are several advantages to using Obukhov length as a stability parameter. It does not contain a mixture of flux and gradient terms, which make R_f difficult to calculate. K_h/K_m is not assumed constant as in Ri. Unlike R_f and Ri, L is independent of measurement height. The main assumptions are the same as those required for Richardson Numbers, i.e., conditions must be reasonably homogeneous in space and stationary in time. The energy divergence and pressure terms of the TKE equation are still ignored. Equation 6.3 for L has the disadvantage that it is composed of covariance terms ($\overline{w'\theta'}$ and u_*) which must be derived from measurements of wind and temperature fluctuations at high data rates using sensitive equipment. Although sonic anemometer/thermometers are capable of these types of measurements, $z/-L$ can also be expressed in a gradient form that permits stability computations using data from less expensive instruments. A gradient form of $z/-L$ is obtained through use of Equations 4.10, 3.3, u_* from Equation 3.12, and defining α as the K_h/K_m ratio, shown by

$$\alpha = K_h/K_m = [(\overline{w'\theta'})/(\partial\overline{\theta}/\partial z)]/[(\overline{u'w'})/(\partial\overline{u}/\partial z)].$$ (6.5)

After simplification, the result is Equation 6.6.

$$z/-L = -\alpha gz(\partial\overline{\theta}/\partial z)\ln(z/z_0)-1)/(\overline{T}\overline{u}(\partial\overline{u}/\partial z))$$ (6.6)

APPENDIX B. REFERENCES

1. Barad, M. L., (Ed.) 1958a: Project Prairie Grass, a field program in diffusion. Vol. I, GRP No. 59, AFCRC-TR-58-235 (I), Air Force Cambridge Research Laboratories, Bedford, Mass. 280 pp.

2. _____, (Ed.) 1958b: Project Prairie Grass, a field program in diffusion. Vol II, GRP No. 59, AFCRC-TR-58-235 (II), Air Force Cambridge Research Laboratories, Bedford, Mass. 209 pp.

3. Biltoft, C. A., 1981: An analytic solution for surface source sigma z calculations. DPG Document No. DPG-TR-81-001. US Army Dugway Proving Ground, Dugway, UT 84022. 20 pp (AD096041.

4. Biltoft, C. A., 1983: A vertical wind angle standard deviation calculation method for the unstable surface boundary layer. DPG Document No. DPG-TR-83-401. US Army Dugway Proving Ground, Dugway, UT 84022. 22 pp. (AD-A132362).

5. Bradshaw, P., An Introduction to Turbulence and its Measurement. Pergamon Press, Oxford, UK, 1971. 218 pp.

6. Businger, J. A., 1973: Turbulent transfer in the atmospheric surface layer. Workshop in Micrometeorology (D.A. Haugen, Ed.), Amer. Meteor. Soc., Boston, MA, 67-100.

7. Businger, J. A., J. C. Wyngaard, Y. Izumi, and E. F. Bradley, 1971: Flux-profile relationships in the atmospheric surface layer. J. Atmos. Sci., 28, 181-189.

8. Calder, K. L., 1949: The criterion of turbulence in a fluid of variable density, with particular reference to conditions in the atmosphere. Quart. J. Roy. Meteor. Soc., 75, 71-88.

9. Caughey, S. J., M. Kitchen, and J. R. Leighton, 1983: Turbulence structure in convective boundary layers and implications for diffusion. Boundary Layer Meteor., 25, 345-352.

10. Cramer, H. E., J. R. Bjorklund, R. K. Dumbauld, J. E. Faulkner, F. A. Record, R. N. Swanson, and A. G. Tingle, 1972: Development of dosage models and concepts. GCA Tech. Rpt No. 70-15-G, US Army Desert Test Center, Fort Douglas, UT. (AD-893-341L)

11. Doran, J. C., T. W. Horst, and P. W. Nickola, 1978: Variations in measured values of lateral diffusion parameters. J. Appl. Meteor., 17, 825-831.

12. Dyer, A. J. and B. B. Hicks, 1970: Flux-gradient relationships in the constant flux layer. Quart. J. Roy. Meteor. Soc., 96, 715-721.

13. Fiedler, B. H., 1984: An integral closure model for the vertical turbulent flux of a scalar in a mixed layer. J. Atmos. Sci., 41, 674-680.

θ_* - temperature scale (degrees Kelvin)

μ - coefficient of viscosity (gram centimeter^{-1} second^{-1})

ρ - density (grams centimeter^{-3})

σ_e, σ_A - vertical and horizontal wind angle standard deviation (degrees or radians)

σ_u, σ_v, σ_w - square root of the variance in horizontal and vertical wind (meters second^{-1})

σ_y, σ_z, σ_x - standard deviations of lateral, vertical, and along wind distributions of diffusing material (meters)

σ_{xt} - component of σ_x due to along-wind fluctuations

τ_0 - surface stress (gram centimeter^{-1} second^{-2})

τ - stress tensor or shear stress (gram centimeter^{-1} second^{-2})

ϕ_m, ϕ_h - dimensionless wind shear and temperature gradient.

χ - concentration (milligrams meter^{-3})

ψ - diabatic influence function (dimensionless)

Ri – gradient Richardson Number (dimensionless)

Ric – Critical Richardson Number (dimensionless)

R_f – flux Richardson Number (dimensionless)

t – time (seconds)

$\overline{T}$ – time-averaged temperature at a specific height (degrees Kelvin)

T' – fluctuating temperature component (degrees Kelvin)

$\overline{u}, \overline{v}, \overline{w}$, – time-averaged wind speeds along the x, y, and z axes (meters second^{-1})

u, v, w, – wind speeds along the x,y,z axis (meters second^{-1})

u', v', w' – fluctuating components of wind speeds along the x, y, and z axes (meters second^{-1})

$\overline{\overline{u}}$ – transport wind speed (meters second^{-1})

u_* – friction velocity (meters second^{-1})

V – vector wind (ui + vj + wk) (meters second^{-1})

x – along-wind travel distance (meters)

z – height of measurement above surface (meters)

z_i – depth of the convective mixing layer (meters)

z_0 – roughness length (meters or centimeters)

α – ratio of K_h to K_m (dimensionless)

ε – turbulent dissipation rate (meters^2 second^{-3})

ε_s, ε_b – rates of turbulent kinetic energy addition by shearing and buoyancy forces (meters^2 second^{-3})

ζ – a variable relating height to wind speed

Δ – delta – indicates an incremental slice or section

λ – wavelength (centimeters)

∇ – del operator ($\vec{i}\,\partial/\partial x + \vec{j}\,\partial/\partial y + \vec{k}\,\partial/\partial z$)

θ – potential temperature (degrees Kelvin)

APPENDIX A. SYMBOLS

A, B - dimensionless constants in the turbulent kinetic energy equation

BU - bulk Richardson Number (dimensionless)

C_N^2 - refractive index structure parameter ($meter^{-2/3}$)

c_p - specific heat at constant pressure (calories $gram^{-1}$ $degree^{-1}$)

D - dose (milligrams)

d - displacement height (meters)

dd - dosage (milligram - minutes/m^3)

E - turbulent kinetic energy ($meters^2$ $second^{-2}$)

f( ) - functional relationship to variable inside brackets

f_c - Coriolis force per unit mass (meter $second^{-2}$)

F_h, F_l - flux of sensible and latent heat (milliwatts $meter^{-2}$)

F_m - flux of momentum (gram $centimeter^{-1}$ $second^{-2}$)

F_x - viscous force per unit mass (centimeter $second^{-2}$)

i, j, k - unit vectors in the x, y, z directions

k - von Karman's constant (dimensionless)

K_h, K_m, K_l - eddy diffusivity for heat, momentum, and moisture
($meters^2$ $second^{-1}$)

L - Obukhov length (meters)

l - length (meters)

ℓ - mixing length or molecular length scale (meters)

n - exponent on power law wind profile (dimensionless)

P - pressure (millibars)

P_{zz} - vertical pressure component (millibars)

Q - source strength (variable units)

R - mixing ratio (milligrams/grams)

RE - Reynolds Number (dimensionless)

b. _Test Data Quality Control_. The similarity theory based equations describing σ_e as a function of gradients obtained from profile data are quite accurate. With high quality data collected at a site of known roughness during quasi-stationary meteorological conditions, the computed turbulence should correspond closely to σ_e obtained from sonic anemometer measurements. Intercomparison of measurements from several tower sites would provide a check on stationary conditions. Discrepancies in excess of 20 percent would indicate that either some equipment was out of calibration or the meteorological conditions were too variable for collection of a coherent turbulence data set.

c. _Posttest Analysis_: The aforementioned instrumentation provides sufficient data for a fairly complete description of meteorological conditions in the SBL. The description begins with incoming/outgoing long- and shortwave radiation from which radiation fluxes can be determined. Near surface scintillation measurements indicate the magnitude of small scale eddy activity generated by radiative fluxes and the decay of larger scale eddies. Eddy activity on this scale deteriorates the performance of all optical instruments. Intermediate turbulence scales, which dominate the turbulence spectrum within a few meters to ten meters of the ground, govern the dissipation rate of substances released into the SBL. Spectrum analysis for this scale of turbulence, along with momentum, heat, and moisture flux/gradient calculations provide the detailed information required for understanding cloud growth and dissipation. The influence of larger scale eddies, which bodily move the cloud without contributing significantly to its dissipation, is obtained from calculation of divergence, analysis of acoustic sounder records, and measurement of mesoscale wind fields. These measurements must then be described within the context of the meso- and synoptic-scale meteorological events taking place. The accumulation of these data should provide the analyst with sufficient information for an in-depth analysis of meteorological conditions influencing a test.

d. _Modeling_. Because L is constant within the SBL, profile data used to calculate L provide sufficient information for model computation of $z/-L$ over the depth of the SBL. Because σ_e is described as a function of z/z_0 and $z/-L$, entire turbulence profiles up to heights of 20 or 30 meters can be achieved using 16-meter tower profile measurements obtained from towers located at representative downwind positions. Supplemented by deeper acoustic sounder wind and mixing depth profiles, these tower measurements could produce the detailed information required for more accurate diffusion models. To accomplish this, methodology work is required to develop better relationships between turbulence calculations or measurements and the diffusion parameters σ_z and σ_x. Further methodology studies are also needed to test alternatives to Gaussian diffusion models.

SBL similarity arguments apply well to the vertical component of turbulence, but are not as useful for describing the horizontal components. Horizontal wind data frequently contain a relatively large amount of energy at low frequencies. These low frequency changes scale with meteorological phenomena occurring above the SBL (such as depth of the convective mixed layer) and are also subject to wind direction trends and terrain influences. No well established algorithms are available to describe these effects. Consequently, horizontal turbulence components are best obtained by direct measurement.

Surface layer similarity arguments described in this document do not apply extremely close to the surface or outside the SBL. The turbulence spectrum near the ground is distorted by the proximity of a fixed boundary which breaks up large eddies. This effect is particularly noticeable for low frequency, high-amplitude eddies which develop during unstable thermal stratification. Because the momentum gradient becomes large very close to the surface, stability near the surface approaches neutral regardless of the intensity of surface heating. Garratt (1980) has developed a methodology for describing near surface conditions, but no conclusive independent testing of this methodology has yet come to the attention of the author. Considerable emphasis has been placed on extending similarity concepts beyond the SBL through the depth of the planetary boundary layer. More work is also required in this area before firm solutions will be available. Future instrumentation needed to probe the planetary boundary layer and beyond will consist largely of remote sensing instruments. These may include lidar wind finding and real-time cloud sampling systems, updated algorithms for acoustic sounder temperature profiles, and FM-CW radar wind sounding systems. Drones may also be used to obtain Lagrangian (moving with the diffusing cloud) as opposed to Eulerian (point measurement) data.

The instruments and similarity theory arguments in this document can provide a vast increase over present DPG turbulence measurement and analysis capabilities. With appropriate displays and data reduction programs, this enhanced capability has the following applications:

a. <u>Test Go/No-Go Criteria</u>. Meteorologists and project officers can use stability information as a quantitative means of evaluating the suitability of meteorological conditions for diffusion tests. Gradients of wind and temperature obtained from tower profile data can be used for real-time calculations of $z/-L$, to assist with test control. For tests requiring near neutral conditions, a $z/-L$ less than 0.03 ($-L$ greater than 67 for $z = 2$ m) is required. When instability up to free convection can be tolerated, a test limitation of 0.35 for $z/-L$ ($-L = 5.7$ m) can be specified. Beyond a value of 0.35 for $z/-L$, buoyancy forces become large and the probability of erratic cloud behavior increases. When $z/-L$ exceeds 1.0 ($-L = 2$ m) buoyancy forces dominate turbulence as mechanical effects steadily decrease. Further increases in instability create a condition of windless convection where horizontal and vertical accelerations are large in comparison to the mean wind field. The erratic looping behavior of cloud plumes occurs under these conditions. Windless convection or other conditions where accelerations become large in comparison to the mean wind field would likely be unsuitable for diffusion testing.

becomes much more difficult at other sites where significant roughness changes occur near the test area. Achieving temporally representative measurements is more difficult because of the short duration (on the order of one to several minutes) of some DPG smoke/obscurant tests. Representative mean values of wind and temperature can be obtained for such short times, but representative variances and covariances require measurements for about 10 minutes. Triple products, such as $\bar{u}'\bar{w}'\bar{w}'$ found in the TKE equation, would required even longer averaging times. Wyngaard et al. (1971) and Wyngaard and Clifford (1978) offer a possible solution that may assist in making temporally representative measurements. Scintillometers provide path-averaged measurements of C_N^2 and wind components. Wyngaard and Clifford suggest that statistically stable samples of path-averaged turbulence data can be collected using only one percent of the averaging time needed for comparable point measurements. A methodology could be developed to take advantage of path averaging techniques for meteorological measurements supporting smoke/obscurant testing.

9. CONCLUSIONS

Useful stability, turbulence, and diffusion measurements can be made if the measurements are made at a reasonable site, with appropriate equipment and proper atmospheric conditions. A reasonable site is relatively homogeneous, with no extraneous obstacles disturbing the turbulence characteristics of the flow. A good site also permits an accurate determination of roughness length, with z_0 independent of wind fetch and a negligible displacement height (d). Appropriate equipment includes an array of 16-meter tall towers instrumented for wind speed and direction at 2, 4, 8, and 16 meters AGL, and a high-frequency turbulence instrument and Lyman-α at 6 meters. The number of instrumented towers required varies with grid size and the degree of homogeneity. Except under extreme diabatic conditions, each tower should be representative of ambient conditions within a several hundred-meter radius at a relatively uniform site on DPG. Tower measurements supplemented by path-averaged winds for divergence and C_N^2 from scintillometers, vertical wind and mixing layer depths from an acoustic sounder, and radiation measurements from precision spectral pyranometers and pyrgeometers would provide a fairly complete set of turbulence data, assuming that the data were collected in a well defined meso- and synoptic-scale setting, and over a sufficient time interval to be representative for the higher moment data required. Additional information on microscale pressure variations is desirable, but difficult to obtain.

The similarity theory arguments presented in this report are valid only for neutral through unstable thermal stratification. A corresponding set of equations has been offered for the stable case, but these equations apply only to stabilities less than the critical Richardson Number (Ric). Oke (1970) states that for stability beyond Ric, the atmosphere is not fully turbulent and there may be no definite forms for profiles of wind and temperature. With clear skies and strong radiation losses, nocturnal stability conditions at DPG almost always exceed Ric. Empirical formulations such as the bulk Richardson Number seem to work as well as anything under these conditions. Consequently, bulk Richardson Number formulations are routinely used for nocturnal diffusion testing at DPG.

of the amount of energy entering and leaving the system. These measurements permit calculation of the radiation balance. Optical instrument tests require these radiation measurements and they are also useful in defining stability categories (Myirski, 1983).

Measurements on the meso and synoptic scale are also needed to describe the setting for diffusion experiments. The presence of fronts, gravity waves, and related phenomena have significant influences on diffusing clouds. These scales of motion are responsible for the transport of diffusing material and generate lee-side eddies which cause diffusing clouds to behave in unexpected ways. Adequate description of meso- and synoptic-scale motions requires an expanded meso-meteorological network and a satellite image receiver.

Test site wind and temperature gradients used for computing turbulence parameters are obtained from fixed point measurements on meteorological towers. The Project Kansas data (Izumi, 1971) indicate that wind and temperature gradients decrease rapidly with height above the surface. Because of the rapidly decreasing gradients, tower profile data above 16 meters contribute little additional information on the conversion of mean flow to turbulent kinetic energy. Consequently, a 16-meter tower instrumented for measuring wind and temperature at 2, 4, 8, and 16 meters AGL should provide sufficient information for gradient computations.

Gradients are computed from profile data averaged over several tens of minutes. Consequently, instrument response time is less critical to good gradient data than accuracy and repeatability. Accuracies approaching 0.01°C and 0.01 m/sec are desired for gradient computations. Such accuracies are approached only when excellent equipment is used and a great deal of care is exercised in the measurement process. Desirable instrument characteristics include freedom from calibration drift, absence of hysteresis effects, and insensitivity to external voltage variations. A high-quality thermal shield and aspiration system is also needed for the temperature measurements. Freedom from external voltage influences is best achieved with sensors that transmit data as frequencies rather than voltages. Well-designed anemometer choppers and quartz crystal thermometers have this desirable characteristic.

Adequate instrument characteristics are necessary but not sufficient for obtaining good wind and temperature gradient data. Wind and temperature must be measured over identical time and height intervals. The geometric mean of profile measurement heights can be used as the height z where $z/-L$ is calculated. The 2-meter level is a good standard level for the lowest profile measurement at DPG because it is not so low that the surface influence significantly distorts the similarity relationships. Measurements closer to the surface should require fast response anemometers. Because diabatic influences usually cause gradients to be nonlinear, multiple measurement points, spaced logarithmically in height, are desirable. Thus, good gradient data could be obtained with profile measurements 2, 4, 8, and 16 meters AGL with a geometric mean z of 5.66 meters.

Having the above mentioned instruments present and collecting data does not guarantee an adequate description of the turbulence field for diffusion tests. The measurements must also be temporally and spatially representative. Achieving spatially-representative measurements is not difficult at DPG, because of the wide expanses of nearly uniform terrain. However, the instruments must not be shaded by man-made obstacles. Spatial representativeness

refractive index structure parameter (C_N^2) which provides a measure of turbulent activity in the small eddy sizes (scintillations). Lawrence et al. (1970) state that optical scintillations are caused primarily by irregularities in the refractive index. The irregularities are variations in air density which have the size of a Fresnel zone, i.e., $(\lambda \ell)^{1/2}$ where λ is a wavelength and ℓ a path length. For visible light and path lengths on the order of a kilometer, eddy size scales causing scintillations are on the order of a centimeter.

Details of eddy activity in intermediate ranges can be obtained by a sonic anemometer. Unlike the LED scintillometer, the sonic anemometer is a fixed-point measurement device. A typical 20-cm path length between probes is the limit of resolution on the small (high frequency) eddy scale. However, in the intermediate size ranges which most strongly influence diffusion on the scale of interest at DPG, the sonic anemometer is able to provide detailed information on the fluctuating wind components (u', v', and w') and the mean wind field, uncompromised by the mechanical damping or overshoot of mechanical vanes. This detailed measurement of the turbulence spectrum is necessary for analysis of the energy in parts of the turbulence spectrum of interest for smoke/obscurant work. Sonic anemometers provide sufficiently detailed data for analysis of the variance and covariance of wind components. This is particularly valuable for obtaining the w components, which are otherwise difficult to measure. Difficulties with sonic anemometers include high cost, the requirements for precision orientation and leveling to prevent cross-component contamination and their electronic complexity. Although discharge anemometers may perform similar measurements, little is known of their characteristics. To obtain moisture flux, a Lyman-α humidity system should be operated concurrently with the sonic anemometer. The product of $\bar{w}'$ with the high-speed humidity measurements will provide moisture flux.

The Doppler acoustic echo sounder is another instrument which provides important turbulence information. This instrument uses the Doppler shift of returning sound pulses to provide mean layer wind information in a vertical profile [and the square root of the variance in horizontal and vertical wind velocity (σ_u, σ_v, and σ_w)]. Additional information can also be obtained on the depth of stable or convective boundary layers (z_i) the height of elevated inversion surfaces. Convective eddy size is largely a function of z_i. Large-scale horizontal variations in wind direction which contribute to the magnitude of σ_A data also scale with z_i (Pasquill and Smith, 1983). Detailed turbulence (σ_u, σ_v, and σ_w) information is best obtained over the depth of a few hundred meters with a high-frequency "mini" acoustic sounder. Mixing height and elevated inversion surfaces aloft require larger, more powerful low frequency units reaching heights near one kilometer. Other instrument systems useful for z_i measurements are described in Kaimal et al. (1982).

For a more complete understanding of boundary layer turbulence, it is necessary to describe the meteorological setting in which turbulence occurs. This setting includes the incoming/outgoing energy that drives this turbulence, which is the long and shortwave radiation and new radiative flux as measured by a set of pyranometers and pyrgeometers. Operating in pairs, with one pyrgeometer and pyranometer facing up and the other facing towards the ground, the amount of long and shortwave radiation passing through a horizontal surface is unambiguously measured. This provides a fundamental measure

Algorithms for determining along-wind cloud growth (σ_x) are less well developed than those for σ_y and σ_z. Wilson (1981) states that except for very close to the source where the plume is small, vertical diffusion and shear advection are the dominant factors determining along-wind dispersion. Wilson offers the following equation for σ_x:

$$\sigma_x = \sigma_z[0.09\ (x \div ((h + 0.5\sigma_z)\ln((h + 0.17\sigma_z)/z_0)))^2 + (\sigma_{xt} \div \sigma_x)^2]^{\frac{1}{2}} \qquad (7.10)$$

where h is the effective source height above the ground in meters and σ_{xt} is the component of σ_x due to horizontal wind fluctuations (u'). Further experimentation is required to refine the algorithms for σ_z (Equation 7.9) and σ_x (Equation 7.10).

8. MEASUREMENT REQUIREMENTS AND INSTRUMENTATION

Adequate description of turbulence in the atmosphere requires knowledge of energies in the spectrum of eddy sizes ranging from the height of the upper boundary (height of the convective mixed layer in the daytime) to the scale at which viscous dissipation begins. Measurements of incoming/outgoing radiative fluxes that initiate diabatic effects are also needed. Although no single instrumented tower provides all of these measurements, point measurement devices can provide a great deal of information about turbulence fields. These instruments must collect data over adequate time and space averages to provide representative measurements. Wind measurements in particular should be taken from multiple locations when fixed point measurement devices such as anemometers and vanes are used. Path averaging devices greatly reduce the instrument deployment requirements.

An important instrument for measurement of turbulent structure is the LED scintillometer (Ochs and Ting-i-Wang, 1978). Scintillometers measure path-averaged wind components perpendicular to scintillometer beam paths. A path-averaged horizontal wind field can be resolved with two beams at right angles to each other. Scintillometers operate over path lengths from 300 to 1500 meters, ideal for most diffusion testing at DPG. Scintillometer path-averaged wind components measured over a triangle can be used to calculate horizontal divergence (Kjelass and Ochs, 1974). For an equilateral triangle, the equation becomes

$$\nabla_h \cdot \vec{V} = 1(V_0 + V_{120} + V_{240})/A = -\partial w/\partial z, \qquad (8.1)$$

where V_0, V_{120}, V_{240} are wind components perpendicular to triangle sides oriented east-west, 30 -210, and 150 -330. Length of the triangle side is 1, and A the enclosed area. Horizontal divergence is related to accelerations in the vertical wind field. Since use of diffusion equations requires the tacit assumption that the atmosphere is nondivergent, divergence measurements may help explain discrepancies between calculations and measured results from diffusion experiments. The LED scintillometer also provides information on the

37

Table 7.2 presents ϕ_m, $B(z/-L)$, and σ_w/u_* for representative values of $z/-L$.

Table 7.2. ϕ_m, $B(z/-L)$, and σ_w/u_* as Functions of $z/-L$ (from Biltoft, 1983).

$z/-L$	ϕ_m	$B(z/-L)$	σ_w/u_*
0.0	1.00	0.00	1.30
0.1	0.80	0.18	1.29
0.2	0.71	0.36	1.33
0.35	0.63	0.63	1.41
0.5	0.59	0.90	1.48
1.0	0.50	1.30	1.72
5.0	0.34	9.00	2.74

Equation 7.7, used in a ratio with the logaritnmic wind-protile (Equation 3.12), satisfies Equation 7.1 to produce a method for computing σ_e

$$\frac{\sigma_w/u_*}{\overline{u}/u_*} = \frac{1.3 \, ((1 + 15 \, z/-L)^{-1/4} + 1.8 \, z/-L)^{1/3}}{[\ln (z/z_0) - \psi]/k} = \frac{\sigma_w}{\overline{u}} = \sigma_e \tag{7.8}$$

Equation 7.8 describes σ_e as a function of stability parameter $z/-L$, height, and roughness. Following Businger (1973), k is assigned the value 0.35. This equation, used with the gradient equation for $z/-L$ derived earlier, permits computation of σ_e for any height within the SBL from wind speed and temperature profile data.

The algorithm

$$\sigma_z = \sigma_e \times f(x) \tag{7.9}$$

is less well established than the one for σ_y. Biltoft (1981) used Project Prairie Grass data (Barad, 1958 a,b) to obtain analytical solutions for σ_z with $f(x)$ a continuous function of cloud travel distance and bulk Richardson Number. As previously mentioned with the σ_y equation, the solutions for σ_z apply to diffusion over 10-minute periods. Adjustments are needed for periods which differ significantly from this. Waldron (1983) has successfully applied these analytical solutions on DPG diffusion tests. Alternative σ_z calculation methods are presented in Pasquill and Smith (1983). Unfortunately, Project Prairie Grass data, which has served as a basis for most σ_z computation methods, did not include adequate σ_e measurements or cloud centroid height information beyond 100 m. Consequently, σ_z values computed for these data are speculative beyond 100 m. More complete data sets are required for a better definition of $f(x)$.

The variance in vertical wind velocity is a Reynolds normal stress component of the TKE equation (Equation 5.25). The TKE equation, with $\partial(\bar{\rho}E)/\partial t$ assumed to be zero and neglecting pressure and flux divergence terms, is reduced to

$$\bar{\epsilon}'/\bar{\rho} = g\,\overline{w'\theta'}/\bar{\theta} - \overline{u'w'}\,\partial\bar{u}/\partial z = \epsilon_s + \epsilon_b \qquad (7.2)$$

Panofsky and McCormick (1960) used this version of the TKE equation with $\bar{\epsilon}'/\bar{\rho}$ defined as $\sigma_w{}^3/zA^3$. Solving for σ_w, the result is Equation 7.3.

$$\sigma_w = A[z(\epsilon_s + B\,\epsilon_b)]^{1/3} \qquad (7.3)$$

A and B are dimensionless constants to be determined below. Constants A and B account for the fact that contributions from shearing (ϵ_s) and buoyant (ϵ_b) kinetic energy do not make equally efficient contributions to the horizontal and vertical components of turbulence. With the aid of Equations 3.3 and 3.11, ϵ_s is described in Equation 7.4, and the relationship between ϵ_s/ϵ_b and flux Richardson Number (from Equation 6.3) is presented in Equation 7.5.

$$\epsilon_s = (\kappa z)^2 (d\bar{u}/dz)^3/\phi_m{}^2 \qquad (7.4)$$

$$\epsilon_s/\epsilon_b = -L\phi_m/z = {}^1/R_f \qquad (7.5)$$

Equations 7.4 and 7.5 are then applied to Equation 7.3. After some algebraic manipulation and division by u_* the result is Equation 7.6

$$\sigma_w/u_* = Ak^{-1/3}(\phi_m + B(z/-L))^{1/3} \qquad (7.6)$$

Following the findings of Biltoft (1983), constants $Ak^{-1/3}$ and B were assigned values of 1.3 and 1.8, respectively.

The dimensionless wind shear term (ϕ_m) in Equation 7.6 is a slowly decreasing function of $z/-L$, whereas the buoyancy term (B $z/-L$) is an increasing function of $z/-L$ (Table 7.2). The combined effect of these terms is that σ_w/u_* remains nearly constant at 1.3 until $z/-L$ reaches a value of 0.35. This is the equilibrium point where shear (ϕ_m) is in balance with buoyancy (1.8 $z/-L$). Beyond this point, buoyancy becomes dominant and σ_w/u_* increases rapidly with $z/-L$. Using Equation 6.8 for ϕ_m, the working expression for Equation 7.6 is

$$\sigma_w/u_* = 1.3((1 + 15\,z/-L)^{-1/4} + 1.8\,z/-L)^{1/3}. \qquad (7.7)$$

described by Irwin (1979) as a complex function of time, Lagrangian/Eulerian time scales, stability, mixing layer depth, release height, and friction velocity.

Table 7.1. Function f(x) for Indicated Downwind Travel Distances and Stability Conditions.

| Stability | Downwind Travel Distance From Point of Release (x, meters) | | | | | |
	100	200	400	1000	2000	3000
Unstable	0.95	0.87	0.7	0.48	0.37	0.3
Neutral	0.8	0.7	0.65	0.42	0.35	0.3
Stable	0.64	0.51	0.45	0.3?	0.32	0.3

Sigma A measurements required for use with the factors in Table 7.1 should be obtained from data collected at a rate of one per second over 10 minutes. For measurements over times significantly different from 10 minutes, adjustments are required (see, for example, Cramer et al., 1972).

Attempts to apply similarity arguments to horizontal wind components have not worked well. Horizontal wind angle data are subject to mesoscale circulations and local terrain influences which impose trends on the data. Direct measurements of σ_A are best. Fortunately, σ_A varies little with height within the constant shear stress layer and the required horizontal wind angle measurements are readily obtained from high quality micrometeorological wind vanes.

The Gaussian diffusion equation describes the vertical growth of a cloud (σ_z) as a function of the vertical turbulence component. This component is often represented as σ_e, the standard deviation of vertical wind angle fluctuations (frequently obtained from bidirectional vane measurements). Experience at DPG with bidirectional vane measurements indicates that these instruments usually operate well when positioned 4 or more meters above the surface, but sometimes fail to produce representative data under extreme diabatic conditions.

In addition to direct measurement, it is possible to calculate σ_e as a function of stability using similarity theory relationships. Sigma e is approximated by the ratio of σ_w (the square root of the variance in vertical wind velocity, $\overline{w'w'}$) to $\bar{u}$, as in Equation 7.1.

$$\sigma_e \simeq \sigma_w / \bar{u} \tag{7.1}$$

Equation 6.6 offers several advantages as a means of describing stability in the SBL. First, it does not contain k. The absolute value of von Karman's constant is not precisely known (see Businger, 1973); accepted values range from 0.34 to 0.41. Second, Equation 6.6 contains no high order gradient terms such as $(\partial \bar{u}/\partial z)^2$ in Equation 5.27 for Ri. This is an important consideration because the gradient terms are the largest source of uncertainty in Ri expressions.

Equation 6.6 requires a specification of α for solution. The term α, shown in Equation 6.5 as the ratio K_h/K_m, is identified by Businger et al. (1971) as the ratio of the dimensionless wind shear (Equation 3.11) to the dimensionless temperature gradient (ϕ_h)

$$\alpha = K_h/K_m = \phi_m/\phi_h = [(kz/u_*)/(\partial \bar{u}/\partial z)]/[(kz/\theta_*)/(\partial \bar{\theta}/\partial z)] \qquad (6.7)$$

where θ_* is a temperature scale analogous to u_*. Businger et al. (1971) used Project Kansas data (Izumi, 1971) to establish empirical relationships between ϕ_m, ϕ_h, and $z/-L$, as represented in Equations 6.8 and 6.9

$$\phi_m = (1 + 15 \ z/-L)^{-1/4} \qquad (6.8)$$

$$\phi_h = 0.74(1 + 9 \ z/-L)^{-1/2} \qquad (6.9)$$

Based on Equations 6.7, 6.8, and 6.9, α is specified as a function of $z/-L$ by the expression

$$\alpha = 1.35(1 + 9 \ z/-L)^{1/2}/(1 + 15 \ z/-L)^{1/4} = \phi_m/\phi_h. \qquad (6.10)$$

With α and (Equation 3.13) specified as functions of $z/-L$, a simple convergence scheme can generate rapid computer solutions for $z/-L$ by using wind and temperature gradient data.

7. STABILITY, TURBULENCE, AND DIFFUSION

As stated in the introduction and further described in Section 4, Gaussian diffusion equations require specification of cloud growth sigmas. Pasquill (1976), with further elaboration by Doran et al. (1978), used field measurements to verify σ_y as a function of horizontal turbulence components (σ_A), travel distance x, and a distance dependent factor $f(x)$ as in Equation 1.2. Function is presented in Table 7.1, based on the findings of Pasquill (1976) and Doran et al. (1978). At distances beyond 1000 m, the neutral case $f(x)$ values were taken to be intermediate between the unstable and stable values, asymptotically approaching 0.3 at extended distances. These numbers represent simplified estimates of turbulence effects. Function $F(x)$ is

33

14. Frenzen, P. 1983: On the role of the flux divergence terms in the turbulent energy production. Sixth Symp. on Turbulence and Diffusion, 22-25 March 1983, Boston, MA. (Amer. Meteor. Soc., Boston, MA).

15. Garratt J. R., 1980: Surface influence upon vertical profiles in the atmospheric near-surface layer. Quart. J. Roy. Meteor. Soc., 106, 803-819.

16. Horst, T. W., 1979: Lagrangian similarity modeling of vertical diffusion from a ground-level source. J. Appl. Meteor., 18, 733-740.

17. Hogstrom, A. S. and U. Hogstrom, 1978: A practical method for determining wind frequency distributions for the lowest 200 m from routine meteorological data. J. Appl. Meteor., 17, 942-954.

18. Irwin, J. S., 1979: Scheme for estimating dispersion parameters as a function of release height. United States Environmental Protection Agency. EPA-60014-79-062.

19. Izumi, U., (Ed.) 1971: Kansas 1968 Field Program Data Report. Environ. Res. Pap. No. 379, AFCRL-72-0041, Air Force Cambridge Research Laboratories, Bedford, MA 73 pp.

20. Kaimal, J. C., N. L. Abshire, R. B. Chadwick, M. T. Decker, W. H. Hooke, R. A. Kropfli, W. D. Neff, and F. Pasqualucci, 1982: Estimating the depth of the daytime convective boundary layer. J. Appl. Meteor., 21, 1123-1129.

21. Kjelass, A. G. and G. R. Ochs, 1974: Study of divergence in the boundary layer using optical propagation techniques. J. Appl. Meteor., 13, 242-248.

22. Lawrence, R. S., G. R. Ochs, and S. F. Clifford, 1970: Measurements of atmospheric turbulence relevant to optical propagation. J. Optical Soc. Amer., 60, 826-829.

23. Mackison, F. W., and R. S. Stricoff, Editors. NIOSH/OSHA Pocket Guide to Chemical Hazards. US Department of Labor US Govt. Printing Office. Washington, DC 1980. DHEW Pub No. 78-210. GPO Stock No. 017-033-00342-4.

24. Monin, A. S. and A. M. Obukhov, 1954: Basic laws of turbulent mixing in the atmosphere near the ground. Tr., Akad. Nauk SSSR Geofiz. Inst., 151, 163-187.

25. Monin, A. S. and A. M. Yaglom, Statistical Fluid Mechanics: Mechanics of Turbulence Vol 1. The MIT Press, Cambridge, MA. 1971. 769 pp.

26. Myirski, M., 1983: A computer program for estimating the vertical diffusion parameters of a chemical cloud released near the surface. ARCSL-TR-83009. US Army Armament Research and Development Command. Aberdeen Proving Ground, MD 21010.

27. Nieuwstadt, F. T. M. and A. P. van Ulden, 1978: A numerical study on the vertical dispersion of passive contaminants from a continuous source in the atmospheric surface layer. Atmospheric Environ., 12, 2119-2124.

28. Obukhov, A. M., 1971: Turbulence in an atmosphere with a nonuniform temperature. Boundary-Layer Meteor., 2, 7-29.

29. Ochs, G. R. and Ting-i-Wang, 1978: Finite aperture optical scintillometer for profiling wind and C^2. Applied Optics, 17, 3774-3778.

30. Oke, T. R., 1970: Turbulent transport near the ground in stable conditions. J. Appl. Meteor., 9, 778-786.

31. Panofsky, H. A. and R. A. McCormick, 1960: The spectrum of vertical velocity near the surface. Quart. J. Roy. Meteor. Soc., 86, 495-503.

32. Pasquill, F., 1961: The estimation of the dispersion of wind borne material. Met. Mag., 90, 33-49.

33. Pasquill, F., 1976: Atmospheric dispersion parameters in Gaussian plume modeling: Part II, possible requirements for change in the Turner workbook values. Report EPA - 600/4-760306. US Environmental Protection Agency.

34. Pasquill, F. and F. B. Smith. Atmospheric Diffusion. John Wiley & Sons, N.Y. 1983. 437 pp.

35. Paulson, C. A., 1970: The mathematical representation of wind speed and temperature profiles in the unstable atmospheric surface layer. J. Appl. Meteor., 9, 857-861.

36. Richardson, L. F., 1925: Turbulence and vertical temperature difference near trees. Philosophical Mag., 49, 81-90.

37. Roberts, O. F. T., 1923: The theoretical scattering of smoke in a turbulent atmosphere. Proc. Roy. Soc. London A., 104, 640-645.

38. Smith, M., 1984: Review of the attributes and performance of 10 rural diffusion models. Bull. Amer. Meteor. Soc., 65, 554-558.

39. Sutton, O. G. Micrometeorology. McGraw-Hill, NY, 1953. 333 pp.

40. Tennekes, H., 1982: Similarity relations, scaling laws and spectral dynamics. Atmospheric Turbulence and Air Pollution Modeling, Edited by F. R. M. Niewstadt and H. van Dop. D. Reidel Publishing Co.

41. Turner, B. D., 1964: A diffusion model for an urban area. J. Appl. Meteor., 3, 83-91.

42. Waldron, A. W., 1983: Verification of predictive surface line source concentration and dosage diffusion models. DPG Document No. DPG-TR-82-007. US Army Dugway Proving Ground, Dugway, UT 84022 (AD 128050).

43. Willis, G. E. and J. W. Deardorff, 1976: A laboratory model of diffusion into the convective planetary boundary layer. Quart. J. Roy. Meteor. Soc., 102, 427-445.

44. Wilson, D. J., 1981: Along-wind diffusion of source transients. Atmos. Environ., 15, 489-495.

45. Wyngaard, J. C. and O. R. Cote, 1971: The budgets of turbulent kinetic energy and temperature variance in the atmospheric surface layer. J. Atmos. Sci., 28, 190-201.

46. Wyngaard, J. C. and R. A. Brost, 1984: Top-down and bottom-up diffusion of a scalar in the convective boundary layer. J. Atmos. Sci., 41, 102-112.

47. Wyngaard, J. C. Y. Izumi, and S. A. Collins, 1971: Behavior of the refractive-index-structure parameter near the ground. J. Optical Soc. Amer., 61, 1646-1650.

48. Wyngaard, J. C. and S. F. Clifford, 1978: Estimating momentum, heat and moisture fluxes from structure parameters. J. Atmos. Sci., 35, 1204-1211.

APPENDIX C. ABBREVIATIONS

AGL - above ground level

CBL - convective boundary layer

DPG - US Army Dugway Proving Ground

NIOSH - National Institute of Occupational Safety and Health

OSHA - Occupational Safety and Health Act

SBL - surface boundary layer

TKE - turbulent kinetic energy

APPENDIX D. DISTRIBUTION LIST

Addressee	Copies

Chairman, Department of Defense
Explosives Safety Board
ATTN: DDESE-KT   1
Forrestal Building
Washington, DC   20314

NOAA Environmental Research Laboratories   1
Wave Propagation Laboratory
325 Broadway
Boulder, CO   80303

Director of Meteorological Systems   1
National Aeronautics and Space Administration
Office of Applications (FM)
Washington, DC   20546

Environmental Protection Agency   1
Division of Meteorology
Mail Drop 80 (J. Irwin)
Research Triangle Park, NC   27711

Director
TRADOC Weather and Environmental
  Support Office
ATTN: ATZL-CAE   1
Funston Hall
Fort Leavenworth, KS   66027

Director
Atmospheric Sciences Laboratory
ATTN: DELAS-AR   1
       DELAS-AT   1
       DELAS-AS   1
       DELAS-AE   1
White Sands Missile Range, NM   88002

Head, Atmospheric Research Section   1
National Science Foundation
1800 G Street, NW
Washington, DC   20550

Department of the Army
Project Manager Smoke/Obscurants
ATTN: AMCPM-SMK   1
Building 324
Aberdeen Proving Ground, MD   21005

Addressee	Copies

National Center for Atmospheric Research   1
NCAR Library
PO Box 300)
Boulder, C⁰ 80303

Commanding Officer
Naval Environment Prediction
  Research Facility
ATTN: Library   1
Monterey, CA 93940

Commander
US Armament, Munitions, and
  Chemical Command
ATTN: AMSMC-ASN   1
Rock Island, IL 61299-6000

Defense Technical Information Center
ATTN: DTIC-DDAC   2
Cameraon Station, Building 5
Alexandria, VA 22304-6145

Commander
US Army Test and Evaluation Command
ATTN: AMSTE-CM   1
       AMSTE-CT   1
       AMSTE-PP   1
       AMSTE-ST   1
Aberdeen Proving Ground, MD 21005

Technical Library   1
Chemical Systems Laboratory
Aberdeen Proving Ground, MD 21010

Acquisitions Section, IRDB-D823   1
Library and Information Service Division, NOAA
6009 Executive Blvd
Rockville, MD 20752

The Library of Congress
ATTN: Exchange and Gift Division   2
Washington, DC 20540

Commander
USAF Geophysics Laboratory   1
ATTN: AFGL-LYT (Mr. Kunkel)
Hanscom Air Force Base, MA 01731

Commander   1
US Air Force Environmental Technical
  Application Center
Scott Air Force Base, IL 62225

Addressee	Copies
Commander Air Weather Service ATTN: MAJ H. Chary Scott Air Force Base, IL 62225	1
US Army Research Office ATTN: DRSRO-PP PO Box 12211 Research Triangle Park, NC 27709	1

Commander
US Army Chemical Research and
  Development Center
ATTN: SMCCR-MSS (M. Myirski)
       SMCCR-SPS-IR
Aberdeen Proving Ground, MD 21010-5423
	1
	1

Commandant US Army Chemical School ATTN: ATZN-CM-CC Fort McClellan, AL 36205-5020	1

Commander
US Army Dugway Proving Ground
ATTN: STEDP-SD
            -MT-DA-M
            -MT-DA-L
            -MT-DA
Dugway, UT 84022
	1
	2
	1
	2

END

FILMED

7-85

DTIC